Synthesis of Co-Doped TiO_2 Nanoparticles using leaf extract of *Millettia ferruginea* for photocatalytic and antibacterial applications

Moges Niguse Woldye

A Thesis Submitted to

The Department of Applied Chemistry

School of Applied Natural Science

Presented in Partial Fulfillment of the Requirement for the Degree of Master's in Applied Chemistry (Physical chemistry)

Office of Graduate Studies

Adama Science and Technology University

June, 2023

Adama, Ethiopia

Synthesis of Co-Doped TiO_2 Nanoparticles using leaf extract of *Millettia ferruginea* for photocatalytic and antibacterial applications

Moges Niguse Woldye

Advisor: Fedlu Kedir (PhD)

Co - advisor: Bedasa Abdisa (PhD)

A Thesis Submitted to

The Department of Applied Chemistry

School of Applied Natural Science

Presented in Partial Fulfillment of the Requirement for the Degree of Master's in Applied Chemistry (Physical chemistry)

Office of Graduate Studies

Adama Science and Technology University

June, 2023

Adama, Ethiopia

Declaration

I hereby declare that this Master Thesis entitled "Synthesis of Co-Doped TiO_2 Nanoparticles using leaf extract of *Millettia ferruginea* for photocatalytic and antibacterial application" is my original work. That is, it has not been submitted for the award of any academic degree, diploma or certificate in any other university. All sources of materials that are used for this thesis have been duly acknowledged through citation.

_____	_____	_____
Name of student	Signature	Date

Recommendation of Advisors

We, the advisor(s) of this thesis, hereby certify that we have read the revised version of the thesis entitled "Synthesis of Co-Doped TiO_2 Nanoparticles using leaf extract of *Millettia ferruginea* for photocatalytic and antibacterial application" prepared under our guidance by Moges Niguse submitted in partial fulfillment of the requirements for the degree of Master's of Science in Applied Chemistry. Therefore, we recommend the submission of revised version of the thesis to the department following the applicable procedures.

_____	_____	_____
Major Advisor	Signature	Date
_____	_____	_____
Co-advisor	Signature	Date

Approval Page

We, the advisors of the thesis entitled "Synthesis of Co-Doped TiO_2 Nanoparticles using leaf extract of *Millettia ferruginea* for photocatalytic and antibacterial application" and developed by Moges Niguse, hereby certify that the recommendation and suggestions made by the board of examiners are appropriately incorporated into the final version of the thesis.

_____	_____	_____
Major Advisor	Signature	Date
_____	_____	_____
Co-advisor	Signature	Date

Approval of Board of Examiners

We, the undersigned, members of the Board of Examiners of the thesis by Moges Niguse have read and evaluated the thesis entitled "Synthesis of Co-Doped TiO_2 Nanoparticles using leaf extract of *Millettia ferruginea* for photocatalytic and antibacterial application" and examined the candidate during open defense. This is, therefore, to certify that the thesis is accepted for partial fulfillment of the requirement of the degree of Master of Science in Applied Chemistry.

_____	_____	_____
Chairperson	Signature	Date
_____	_____	_____
Internal Examiner	Signature	Date
_____	_____	_____
External Examiner	Signature	Date

Finally, approval and acceptance of the thesis is contingent upon submission of its final copy to the Office of Postgraduate Studies (OPGS) through the Department Graduate Council (DGC) and School Graduate Committee (SGC).

_____	_____	_____
Department Head	Signature	Date
_____	_____	_____
School Dean	Signature	Date
_____	_____	_____
Office of Postgraduate Studies, Dean	Signature	Date

Acknowledgement

First, I give all glory and honor to the supreme God, the source of all wisdom, knowledge and understanding. I am thankful to my advisors Dr. Fedlu Kedir and Dr. Bedasa Abdisa for their constructive comments, encouragement and assistances for accomplishing this research thesis. My acknowledgement is also extended to Dr. Lemma Teshome for his valuable support during samples characterization.

I would like to thank Adama Science and Technology University for giving me this scholarship program to endure my academic career.

I would like to thank Department of Applied Chemistry and Department of Material Science and Engineering, Adama Science and Technology University for letting me use the laboratory with its chemicals, materials, and instruments necessary for the work. In addition, I want to thank Mr. Guta, Mr. Lemi, and Mr. Demeke for giving me the information, help, and resource I needed to carry out my research.

Last but not least, I want to express my sincere gratitude to my family for always being there for me. My sincere gratitude also extends to Mr. Getye, Mr. Yinebeb, and Mr. Hailemikael for their kind assistance, support, and guidance in various ways.

Table of Contents page

List of Tables

List of Figures

List of Abbreviations

AOPs	Advanced oxidation process
CB	Conduction band
DMSO	Dimethylsulfoxide
DTA	Differential thermal analysis
DW	Distilled water
EAOPs	Electrochemical advanced oxidation processes
FTIR	Fourier-transform infrared spectrometer
MB	Methylene blue
MNPs	Metallic nanoparticles
MONs	Metal oxide nanostructures
MRI	Magnetic resonance imaging
NMs	Nanomaterials
NPs	Nanoparticles
NSs	Nanostructures
SEM	Scanning electron microscope
TGA	Thermogravimetric analysis
TTBO	Titanium tetra-butoxide
VB	Valence band
UV	Ultraviolet
UV-Vis DRS	UV–Vis diffuse reflectance spectroscopy
XRD	X-ray diffraction

Abstract

Photocatalysis is an efficient technique for reducing environmental contamination caused by organic pollutants. The present study investigated the photocatalytic and antibacterial activity of nanomaterial composed of Titanium Oxide (TiO_2), and cobalt doped Titanium oxide (Co-doped TiO_2). TiO_2 and Co-doped TiO_2 nanomaterials were synthesized in greener way using cheap and easily available Ethiopian endemic plant extract known as Millettia ferruginea. This green and plant templated method of nanomaterial synthesis avoids using hazardous chemicals and use ecofriendly plants extract. The synthesized materials were characterized by thermogravimetric analysis (TGA), X-ray diffraction (XRD), UV–Vis diffuse reflectance spectroscopy (UV-Vis DRS), Fourier transform infrared (FT-IR) spectroscopy, and scanning electron microscopy (SEM). The synthesized undoped TiO_2, 2% Co-doped TiO_2, 4% Co-doped TiO_2, and 6% Co-doped TiO_2 were investigated for their photocatalytic activity against methylene blue (MB) dye. Among them, the 6% Co-doped TiO_2 Nanoparticle was found to be better photocatalysts with adigradation efficiency of 93.4% under visible light irradiation. Further, parameters such as effect of pH of the dye solution, catalyst loading and initial dye concentration were also studied and optimum degradation efficiencies were found at pH 9, catalyst load of 20 mg, and with dye concentration of 10 ppm. The synthesized TiO_2 and Co-doped TiO_2 nanomaterials were also applied against Gram-negative (E. coli and P. aeruginosa) and Gram-positive (S. aureus and S. pyogenes) bacterial strains to evaluate their antibacterial activities. The 6% Co-doped TiO_2 Nanoparticles was shown to have better inhibition zone against all tested bacterial strains except S. aureus when compared to other synthesized nanomaterials for antibacterial activity.

***Keywords*:** Titanium oxide, Cobalt doped Titanium oxide, Antibacterial activities, photocatalytic degradation, and methylene blue.

1. Introduction

1.1 Background

Nanotechnology is a branch of science that concerns on the creation, manipulation, and control of nanoscale materials known as nanomaterials. Nanomaterials are materials with at least one of their dimension is less than 100 nm length and differ from their bulk counterparts in terms of optical, electrical, and catalytic characteristics (Feiona et al., 2021; Jalab et al., 2021). Based on their physicochemical properties, these materials have a wide range of applications in domains such as energy conversion and storage (Anigol et al., 2017); medicine, and pollution remediation. The chemical, physical, electrical, and optical properties of nanomaterials are all influenced by particle size, shape, and surface morphology (Annu & Ahmed, 2018).

Nanoparticles (NPs) are zero dimensional particles with all the three dimensions in the range of 1 to 100 nm size. NPs can be used as medium of transportation for drug delivery in cancer treatment due to its high bioavailability, efficiency and improved permeability (Osonga et al., 2020). Nanostructures (NSs) have a potential application in water and air pollution reduction, energy production, and as antibacterial and anti-viral agent. Now days, metal oxides nanostructures (MONSs) gets more attention due to their novel optical, electronic, magnetic, thermal, catalytic and mechanical properties in comparison with their bulk materials (Shanaj & John, 2016). As a result, MONSs were studied and found to be applicable in catalysis, medical science including antibacterial, antiviral, and anti-carcinogenic and for fabrication of sensor, semi-conductor and capacitive electrodes (Ismail, Hasoon, & Saheb, 2019).

The essence of water in our lives can be understood from the fact that no living being can survive on the earth without water. However, water pollution has become a global concern because of the increased addition of different industrial contaminants to drinking water reservoirs (Javed et al., 2021). The textile industries, for instance, use highly reactive dyes, such as methylene blue and methyl orange, which are harmful to the environment due to their high carcinogenic and mutagenic potential. When discarded without adequate treatment, they can change the color of water bodies, promoting significant changes in the hydrological cycle (Nassar et al., 2016). So far, traditional approaches have been adopted to address those problems, like adsorption (Liu et al., 2020), membrane filtration (Yang et al., 2020), coagulation/flocculation (Yogalakshmi et al., 2020), oxidation or ozonation (Sicardi, 2020), reverse osmosis (Pype et al., 2016), and so on. However,

these methods cannot completely remove or ineffectively remove organic pollutants in water. In recent years, photocatalytic degradation of wastewater is a promising way owing to efficiency, green, environmental compatibility and convenience. Photocatalytic reaction is a heterogeneous reaction that occurs on the catalyst surface to accelerate the conversion of light energy into chemical energy, including excitation, redox reaction and recombination, and to achieve the potential balance between the Fermi energy level of the catalyst and the surface adsorbents (Bai et al., 2021).

The core of photocatalytic technology is to find and design suitable photocatalyst. Among various photocatalysts, TiO_2 is one of the most widely investigated semiconductor photocatalysts in the field of water treatment because of its good chemical stability, low toxicity, abundance, inexpensive, and ease of preparation. However, TiO_2 exhibits photocatalytic activity and high oxidizing power only in UV-light due to its high band gap energy (3.2 eV) this can limits its photocatalytic activity in visible light. In the recent years, Doping plays a significant impact on nano TiO_2 semiconductor photocatalysis. Dopants alter the electronic structure of the nano TiO_2 to extend its potential range of light sensitivity from UV-region to visible light region for photocatalysis (Lakshmi et al., 2018).

Several main group elements, and transition metals have been utilized as dopants for TiO_2 NPs arrays with varying degrees of success. Among the transition metals, cobalt has been especially applied as a TiO_2 dopant for several applications. For instance, Co-doped TiO_2 has shown remarkable success as a catalyst in the decomposition of inorganic pollutants, the oxidation of cyclohexane and the degradation of complex organic dyes (Venturini et al., 2019).

Several methods have been used for metal oxide nanoparticles synthesis such as hydrothermal, wet chemical, microwave method, co precipitation, sol–gel, and thermal decomposition. However, these classical methods to synthesize metal oxide nanoparticles using hazardous chemicals has a negative effect for the ecology of our environment. As a result, green synthesis of metal oxide nanoparticles and metal-doped nanomaterials has received special attention due to a cheaper and environmentally friendly method. This green method of synthesis refers to the formation of nanoparticle structures which are capped by organic materials from living organisms or plants (Seabra & Durán, 2015). Here in, Co-doped TiO_2 NPs were synthesized using *Millettia ferruginea* leaf extract as stabilizing and capping agents for degradation of organic dye.

1.2 Statement of the problem

An increasing demand for resources globally causes energy crises and environmental pollution. Industrialization which is progressively increased to fulfill the demand of the community contributes to water pollution by the release of organic and inorganic pollutants (F. Zhang et al., 2019).

TiO_2 NPs is a good candidate for photocatalytic degradation of organic pollutant because of its low cost, high photosensitivity, and nontoxic nature (L. Wang et al., 2013). However, the rapid charge carrier recombination and wide band gap of TiO_2 limit its photocatalyst efficiency. As a result, surface modification of TiO_2 NPs by doping with metal or nonmetal elements are the best method to overcome the challenges. Cobalt is an excellent light absorber in the visible range, so the addition of cobalt to TiO_2 NPs improves their photosensitivity and photocatalytic efficiency. In this work, cobalt was used as dopants in TiO_2 NPs and the products were characterized by various analyses. Also, antibacterial and photocatalytic activities of this product were investigated.

Green method is the best method to synthesize Co-doped TiO_2 NPs due to low cost, environmental friend, and easily manageable routes. Green synthesis of Co-doped TiO_2 NPs using different plants extracts was reported. But to the best of my knowledge, synthesis of Co-doped TiO_2 NPs through the green route by using *Millettia ferruginea* leaf extract was not reported before this work. Therefore, in this study the leaf extracts of *Millettia ferruginea* was used as reducing, stabilizing and capping agents for synthesis of Co-doped TiO_2 NPs.

Bacterial infectious diseases are serious health problem that has drawn the public attention in worldwide as a human health threat, which extends to economic and social complications. Increased outbreaks and infections of pathogenic strains, bacterial antibiotic resistance, emergence of new bacterial mutations, lack of suitable vaccine in underdeveloped countries, and hospital associated infections, are global health hazard to human. Antibacterial resistance has emerged as one of the biggest threats to human health globally due to the over use of antibiotics. Due to development of drug resistance in pathogenic bacteria, the commonly treated illnesses yesterday are becoming lethal today. Hence, new strategies and approaches are highly demanded to take the major health care challenge posed by rapidly spreading antibiotic resistant bacteria (Rojas-Andrade et al., 2017). So, in this study, TiO_2 and Co-doped TiO_2 NPs were synthesized using

environmentally friendly methods, and their photocatalytic and antibacterial activity were examined.

1.3 Objectives

1.3.1 General Objective

The general objective of this study was:

To synthesize Co-doped TiO_2 nanoparticles and evaluate its photocatalytic, and antibacterial activity.

1.3.2 Specific Objectives

The specific objectives of this research were:

- To synthesize Co-doped TiO_2 NPs through green method using leaf extract of *Millettia ferruginea*.
- To characterize the synthesized nanomaterials using TGA, XRD, UV-Vis DRS, FTIR, and SEM characterization techniques.
- To evaluate the photocatalytic activity of synthesized nanomaterials for the removal of methylene blue (MB) dye from aqueous solution.
- To test the anti-bacterial activities of synthesized nanomaterials against human pathogens such as Gram-negative (*Escherichia coli, and Pseudomonas aeruginosa*) and Gram-positive (*Staphylococcus aureus, and Streptococcus pyogenes*) bacterial strains.

1.4 Significance of the study

This study would provide methods to overcome problems such as band gap widening and electron hole recombination by using doping with cobalt. The outcome of this study could be used to benefit the society considering the need of pure water. This study provided information about the antibacterial activity of TiO_2 NPs and Co-doped TiO_2 NPs.

1.5 Scope of the study

This study was covered the synthesis of TiO_2, and Co-doped TiO_2 NPs through green method using leaf extract of *Millettia ferruginea*. The properties of synthesized NPs were characterized using thermogravimetric analysis (TGA), X-ray diffraction (XRD), UV–Vis diffuse reflectance spectroscopy (UV-Vis DRS), scanning electron microscopy (SEM), and Fourier transform infrared spectroscopy (FT-IR) techniques. The NPs were evaluated for antibacterial activity against human

pathogens such as Gram-negative (*Escherichia coli, and Pseudomonas aeruginosa*) and Gram-positive (*Staphylococcus aureus, and Streptococcus pyogen*) bacterial strains. The photocatalytic activities of synthesized NPs were tested for degradation of MB pollutant dye in aqueous solution. The mechanism of photocatalytic degradation of MB through TiO_2 and Co-doped TiO_2 NPs was studied using pseudo first and pseudo second order kinetic models.

2. Literature Review

2.1 Nanoparticles

Researchers are currently focused on designing nanoparticles to modify their electronic, optical, catalytic, and magnetic properties, irrespective of the properties of the bulk materials. The key factors in achieving this are quantum effects and surface area, which require careful consideration in order to effectively tune the properties of the nanoparticles. Extensive researches have been carried out to control the shape and size of NPs since size and shape have significant effect on physico-chemical properties (N. T. Khan & Khan, 2020). Nanoparticles are generally defined as particulate matter with at least one dimension that is less than 100 nm. This definition puts them in a similar size domain as that of ultrafine particles (air borne particulates) and places them as a sub-set of colloidal particles. These particles are interesting, as they show unique and considerably different physical and chemical properties compared with their macro scaled counterparts (Patra & Baek, 2014). Better properties, such as catalytic, magnetic, electro-mechanical, optical, chemical and biological properties are displayed at nano scale. The higher strength, reactivity, mobility, enzymatic and chemical activity, and dissolution properties are properties that shown by NPs as a result of their high surface are (Sahoo et al., 2021).

NPs have a wide range of applications in areas such as medicine, electronics, energy, and environmental remediation. In medicine, NPs are being developed as drug delivery systems, imaging agents, and diagnostic tools. They can be designed to target specific cells or tissues in the body, and can be used to enhance the effectiveness of drugs while reducing side effects. In electronics, NPs are being used to develop smaller and more efficient devices, such as transistors and memory chips. They are also being used in solar cells to increase the efficiency of energy conversion. NPs are also being used in environmental remediation to remove pollutants from water and air. They can be designed to bind to specific pollutants, such as heavy metals or organic compounds, and can be used to remove them from contaminated sites (Kumar Teli et al., 2010). On the basis of constituent, NPs could be classified under organic and inorganic NPs. Organic NPs are those synthesized from polymer and lipid based precursors. The constituent of inorganic NPs are metalllic and metal oxide precursors(Sahoo et al., 2021).

2.2 Synthesis Method of Nanoparticles

The conventional methods for the synthesis of NPs can be broadly classified in two different approaches, i.e. top-down and bottom-up (Figure 1). In top-down approach, NPs are formed by size reduction method that means suitable bulk material reduces to small units with the use of appropriate lithographic methods, for crushing, spitting, and milling (Siavash Iravani, 2011). The bottom-up approach involves the generation of NPs from small units like molecules and atoms or through the self-assembly of atoms into new nuclei, which further grow into a particle possessing nanoscopic dimensions and employing various chemical and biological methods (Mittal, Chisti, & Banerjee, 2013).

The bottom-up approach has gained interest due to its advantage of size and structural control in the synthesis of NPs. However, the chemical methods are cost-effective, mass production is limited, requires high energy, high temperature and pressure, uses toxic and volatile reagents that cause a hazard to the environment and human life. So, the scientific community has explored a new method of synthesis of NPs that is a biological method, which is environmentally benign, non-toxic, uses less expensive chemicals, and requires low energy for cost-effective production (Karthikeyan et al., 2017).

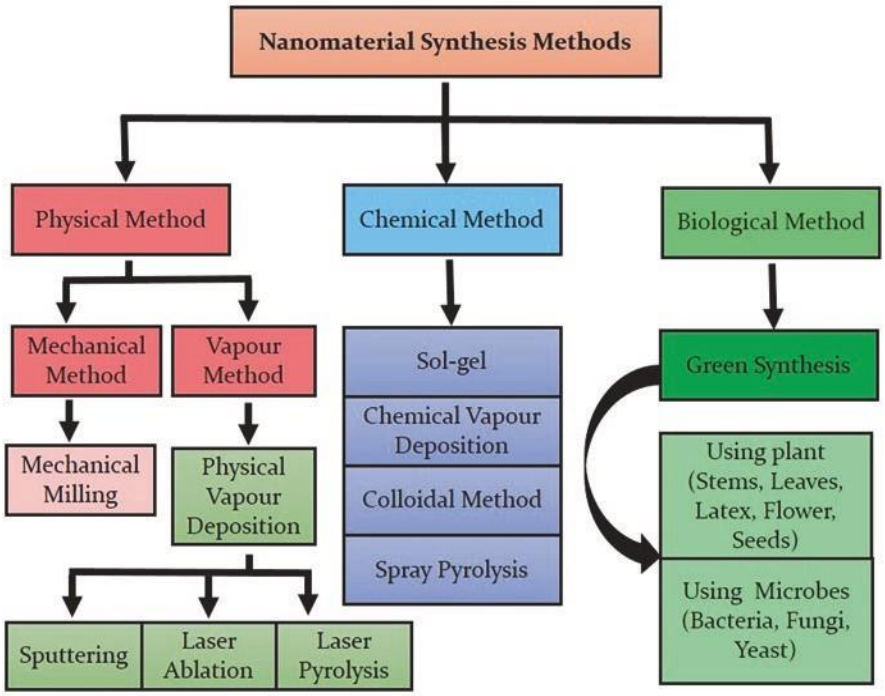

Figure 1: Synthesis methods for nanoparticles (Goutam et al., 2020)

On the other way, three different strategies of synthesis of NPs are commonly known. These are the physical, chemical and green methods. In the physical method, physical forces are involved in the attraction of nano scale particles and formation of large, stable, well-defined nanostructures. The physical method often called top-down approach. It uses mechanical forces to break bulk particles or beams of atoms for the formation of NPs. The physical method for NPs synthesis includes milling, vapour phase synthesis, mechanical grinding, evaporation-condensation, ion implantation, arc discharge method, electron beam lithography, inert gas synthesis and the laser ablation methods. In evaporation condensation method, the tube-furnace at atmospheric pressure is brought to use (Abou El-Nour et al., 2010), and as per the name, the source material gets converted into carrier gas, respectively.

The chemical method involves the use of toxic chemicals which can prove to be hazardous for the environment and the person handling its surface. The chemical method of nanoparticle synthesis comprises of methods like electrolysis, pyrolysis, co-precipitation method, sol gel process, solvothermal synthesis, chemical reduction of metal salts and phytochemical irradiation method. The co-precipitation method of nanoparticle synthesis is one of the most commonly used methods which involve the addition of base in the aqueous salt solutions under inert atmospheric conditions. Sol-gel method is mostly used for generating the metal oxides and conversion of the source material into a sol i.e. a colloidal solution, which acts as the 'precursor' of the complexed network of gel (Siavach Iravani et al., 2014). It all includes the use of reducing agents that can be both organic and inorganic, like ascorbate, citrate, elemental hydrogen and borohydride. In this approach of synthesis, nanoparticles generally possess different parameters because of the reduction of the metal ion in various aqueous mixtures; thus, for stabilizing these NPs, many 'protective agents' including vinyl alcohol, vinyl pyrrolidone, ethylene glycol, meth-acrylic acid and polymethyl methacrylate have been reported to be used (S. Ahmed et al., 2016).

Green/biosynthesis of NPs is an approach of synthesizing NPs using microorganisms (bacteria, fungi, algae) and plants (leaves, flower, seed and peels) as the reducing and stabilizing agents for synthesis of NPs instead of large quantity of chemicals. This method does not require high temperature, high pressure, costly equipment and hazardous chemicals. Due to their cost effectiveness, these synthesis method have been the subject of widespread interest. It provides the benefits of less time consumption along with very less monetary expenses involved for

biosynthesis of NPs. Many different unicellular and multi-cellular living forms such as actinomycetes, yeast, bacteria, fungi, algae, plant extract and enzymes are being used for nanoparticle synthesis. Large-scale production of NPs occurs via green approach (Shah et al., 2015).

2.2.1 Green Synthesis of Nanoparticles

Green synthesis is commonly used for the production/fabrication of NPs. The advantage of this methods is that they are simple, facile, and environmentally friendly, and the synthesized nanomaterials are nontoxic and biocompatible. NPs with definite size and shape can be produced by adjusting the concentration of reducing agent, temperature, and PH. Around the world, green routes (simple, eco-friendly, and emerging approach) based on bioassisted materials have become a promising technology for the synthesis of various nanoparticles. Moreover, this approach is devoid of outdated, eroding, toxic, and combustible reducing agents (e.g., BaBH4). Green process is widely used for TiO_2 involved the use of either plant extracts or microbes (bacteria, fungi, etc.) (Figure 2) (Rani & Shanker, 2020).

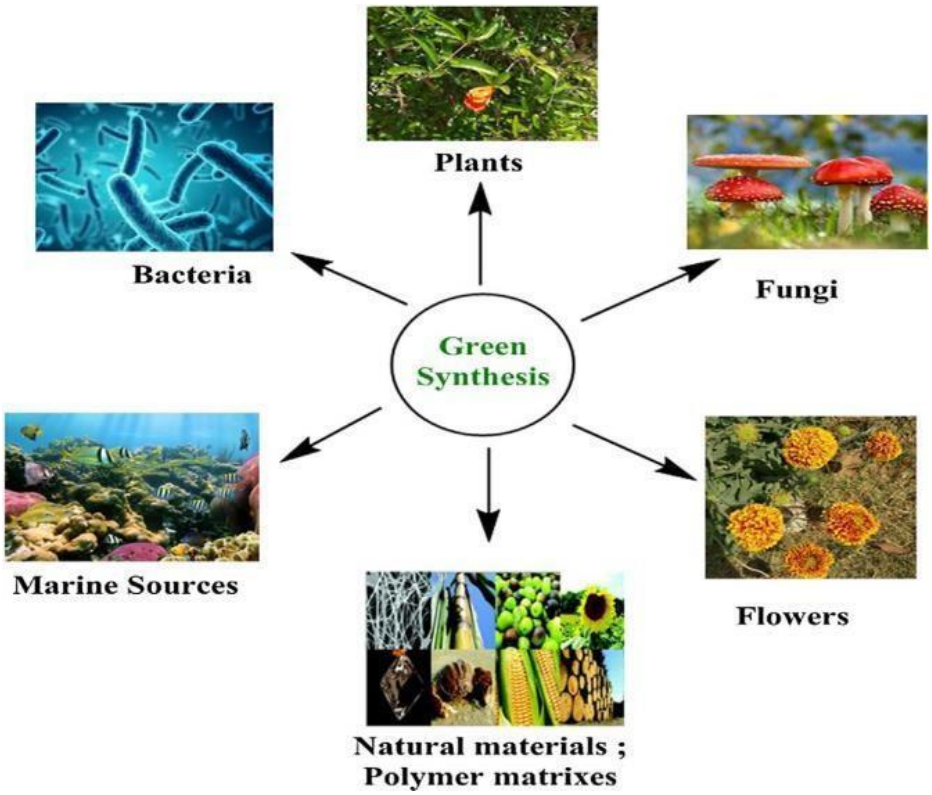

Figure 2: Strategy for green synthesis of nanomaterials (Rani & Shanker, 2020)

2.2.1.1 Synthesis of Nanoparticles from bacterial and fungal extract

Both fungal and bacterial extracts have been utilized for the biosynthesis of NPs. The metabolites in bacterial biomass may help in stabilizing and bio-reducing the NPs. Moreover, as compared to bacterial extract, fungal extract has been given considerable attention based on advantages of simple extraction, large scale production, economic feasibility and increased surface of synthesized NPs. Different sizes and shapes of TiO_2 NPs have been reported as fungus constitutes enzymes and metabolites which make them able to carry out the deduction of bulk salts into elements of ions (Nadeem et al., 2018). Previously, TiO_2 NPs were synthesized from a bulk TiO_2 precursor by employing *Aspergillus tubingensis* fungi (Tarafdar et al., 2013).

Bacterial-assisted synthesis of NPs can be done through two approaches: intercellular and extracellular approaches. The intercellular approach is time consuming, so the extracellular approach is widely used because it takes less time as it does not need any downstream process for the collection of NPs from the organisms (Vinatier et al., 2009). Previously, different researchers made use of bacteria as a reducing and a capping agent to control the grain/overgrowth during the synthesis of TiO_2 NPs and other nanomaterials having various applications. A cost effective biosynthesis method involving *Acinetobacter baumannii* was studied for improved photocatalytic dye treatment with 78% efficiency in short time with only 0.3 g TiO_2. Bacteria including *Aeromonas hydrophila*, *Lactobacillus sp.* and *Bacillus subtilis* bacteria were observed for simple, easy, reproducible, and cost-effective synthesis of TiO_2. Also, mass production of TiO_2 NPs did not require costly chemicals, high pressure and temperature (Fulekar et al., 2018). The technique was identified to be advantageous as it was observed to be the simple green synthesis approach with significant activity of prepared NPs (Jayaseelan et al., 2013).

2.2.1.2 Synthesis of Nanoparticles using plant extract

Even though different microorganisms have been employed as an alternative template for the synthesis of nanomaterials instead of using expensive and toxic organic solvents and chemicals as a stabilizer, the use of microorganisms has its own disadvantages as compared to medicinal green plants as they require advanced equipment and instruments to culture and enhance their growth before they are used for synthesis purpose and require optimization of different parameters to achieve and maintain their growth and to be used during the synthesis process. Instead, incorporating different parts of green and medicinal plants results in to ecofriendly benefits to the

ecosystem. Due to the diversity of plants, NPs synthesis from plant extract has known as an interesting subject across the world as different plant species are being rapidly investigated and used in NPs synthesis (Taoda et al., 2008).

Commonly, the advantages of safety and feasibility make the plant extract as the key component for the NPs synthesis. Plants contain proteins, carbohydrates, enzymes as well as phenolic acids and alkaloids which carry out reduction and stabilization processes in the synthesis. Plant extracts can be generally obtained from any part of the plants, namely flowers, roots, seeds, and leaves. The desired part of the plant from where the extract has to be obtained is thoroughly washed and then boiled in solvent (ethanol or distilled water) for a few min followed by filtration. The resultant filtrate is the plant extract to be used as a reducing agent to which a suitable metallic precursor is added with constant stirring to obtain NPs (Irshad et al., 2022; Jadoun et al., 2021).

2.3 Metallic Nanoparticles

The existence of metallic nanoparticles (MNPs) in the solution was recognized by Faraday in 1908. The quantitative explanation of these NPs was given by Mie in relation to the colour of the NPs (Kumar et al., 2018). MNPs, which could be synthesized by the reduction of metal from metal salt solution or formation of metal atom aggregates by vaporization or heating a metal in the presence of inert gas or at vacuum are known for their surface Plasmon resonance and high surface area to volume ration, uniform size and sharp size distribution, all makes interesting for nanotechnology applications (Nakamura et al., 2019). Synthesis of MNPs could be using top-down or bottom-up approach with different specific technique within each approach (Figure 3) (Jeyaraj et al., 2019).

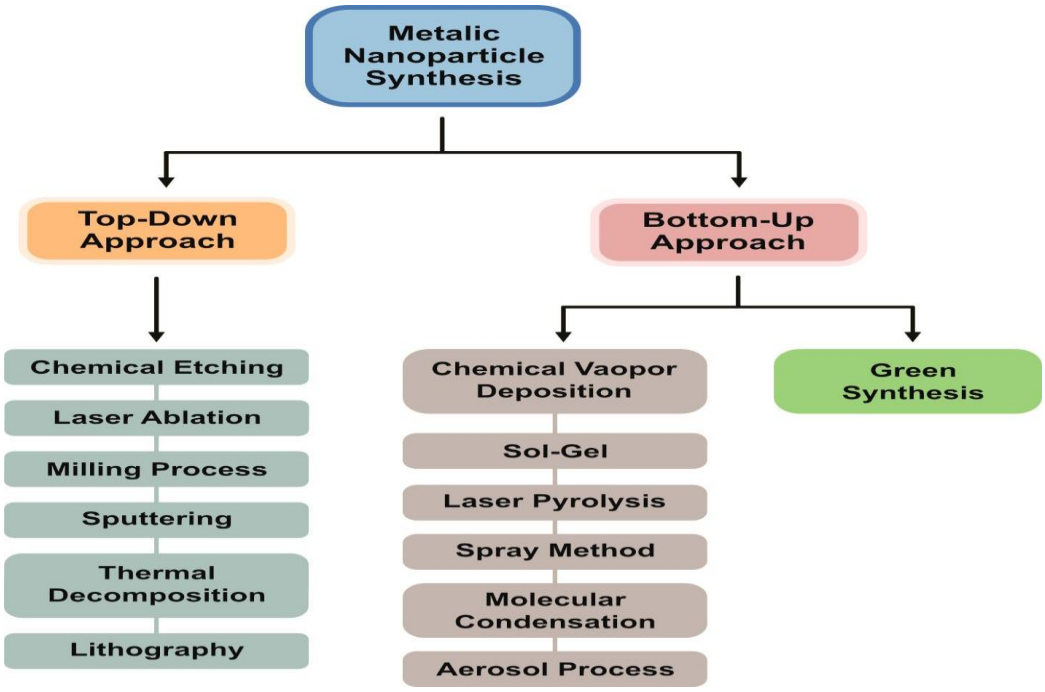

Figure 3: Synthesis approaches of metallic nanoparticles (Jeyaraj et al., 2019)

A bottom-up approach is the build-up of nanostructures from the smaller starting materials which can be atom-by-atom or molecule-by-molecule development by physical and chemical methods. In top-down approach, the breaking down of bulk material is essentially carried out to get nanoparticles. This can be achieved through advanced techniques such as precision engineering and lithography (Bayda et al., 2019).

MNPs are applicable in various fields of science related to health, environment and electronics. The common applications of MNPs are depicted in Figure 4 (Simões et al., 2020). MNPs may answer challenges in environment and industries by increasing the utilization of solar energy, fabrication of catalyst, using as drug carrier and water pollution.

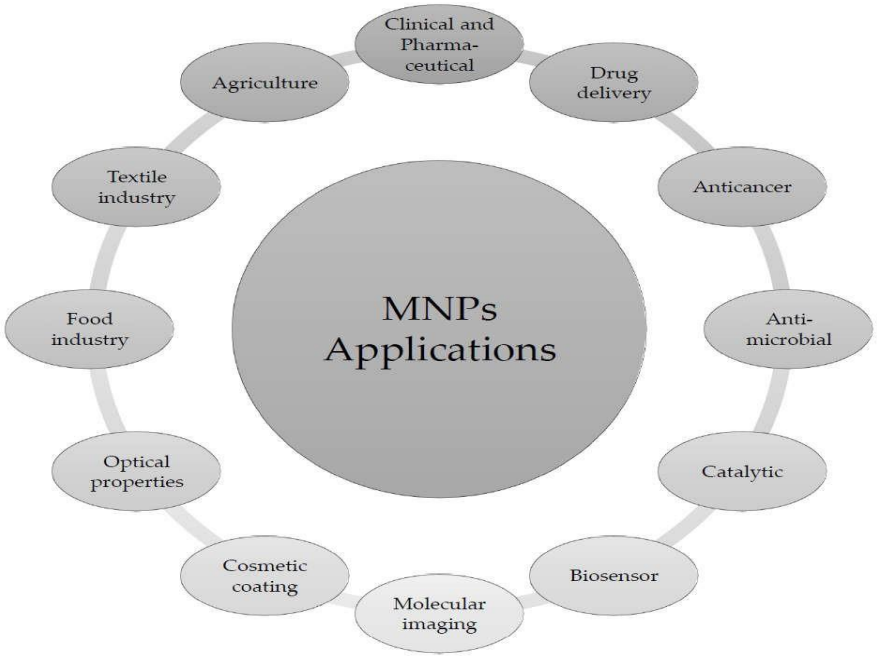

Figure 4: Applications of Metal nanoparticles (MNPs) (Simões et al., 2020)

2.3.1 Titanium Oxide Nanoparticles

Titanium Oxide (TiO_2) is a transition metal oxide that has outstanding thermal, electrical, optical, and semi-conductive properties and is found naturally in oxide form, which makes them suitable aspirant for a number of applications. TiO_2 is a white, crystalline powder and usually insoluble in water under normal conditions. It is a highly stable material and is mostly used as an opacifier (Panhwar et al., 2021).

In recent decades, the most comprehensively studied metal oxides have been titanium oxide (TiO_2) nanoparticles. Owing to its photostability, reasonable price, high photocatalytic activity, and biological and chemical stability (Guesh et al., 2016), TiO_2 is to date the most exceptional photocatalyst. Usually, charge separation within particles is induced in TiO_2 because of the large bandgap energy (3.2 eV) and ultraviolet (UV) excitation. TiO_2 nanoparticles possess little selectivity, which makes these nanoparticles suitable for the degradation of all kinds of contaminants, such as polycyclic aromatic hydrocarbons (Guo et al., 2015), chlorinated organic compounds (Dubey et al., 2021), dyes (Sathiyan et al., 2020), pesticides (Budarz et al., 2019), phenols (Zamri & Sapawe, 2019), cyanide (Ijadpanah-Saravi et al., 2016), and heavy metals (Donga et al., 2021). The photocatalytic properties of TiO_2 nanoparticles can kill a wide array of

microorganisms, such as gram-positive and gram-negative bacteria as well as viruses, algae, fungi, and protozoa (Verma et al., 2022).

Titanium has a huge number of potential applications (Figure 5) in various fields, including food, paint, cosmetic, paper, and pharmaceutical industries. Being a semiconductor material, it is widely used in technological fields to make capacitors, electrochemical electrodes, solar cells and shows excellent photocatalytic activity towards many reactions. Furthermore, it is used for dye-sensitized fuel cells, water splitting, and removing various organic contamination from aqueous media (Jassal et al., 2022).

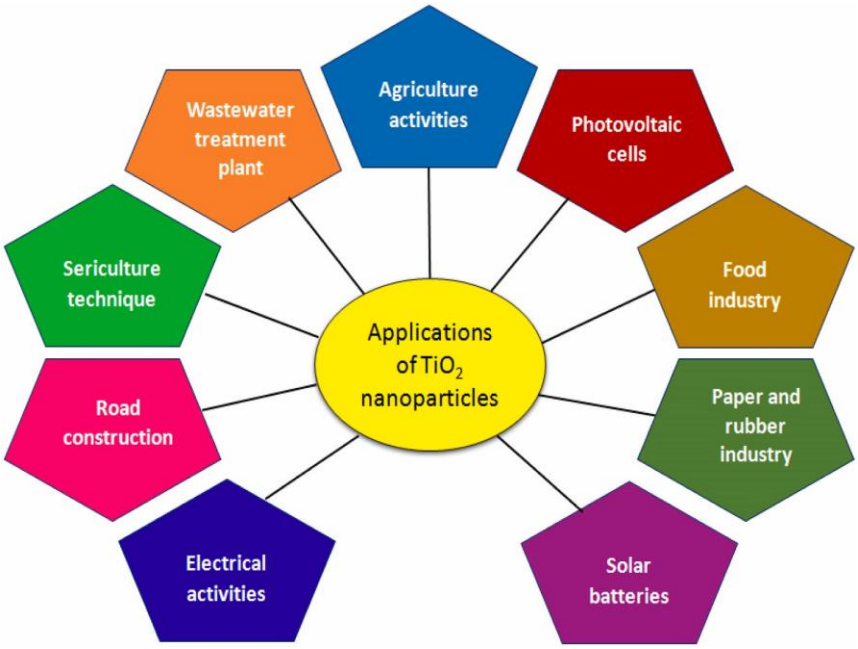

Figure 5: Applications of Titanium oxide nanoparticles (Jassal et al., 2022)

TiO_2 has three major crystalline forms, i.e., anatase, rutile and, brookite. Anatase and rutile forms of titania possess almost similar properties which include, luster, hardness, density, and interestingly, they have identical structural symmetry (tetragonal). The pure form of rutile and anatase can be synthesized at low temperatures and are preferred for the photocatalytic process. TiO_2 nanometal is relatively less expensive than any other nanomaterial and exhibits good thermal and chemical stability and low human toxicity. In addition to their photocatalytic properties, they are widely used in wastewater purification and anti-biofouling. The main advantage of TiO_2

nanoparticles is that they have an endless lifetime and remain unchanged during the degradation process of microorganisms and organic compounds (Liou & Chang, 2012).

2.3.2 Cobalt Oxide Nanoparticles

Cobalt, a d-block transition metal, is mainly deployed in paint and ceramic industries (I. Khan, Saeed, & Khan, 2019), and its compounds are often used as catalysts in an array of organic reactions namely hydro-formylation, hydrogenation, and dehydrogenation reactions, among others. Cobalt has quite a few beneficial effects when it comes to human health, being part of vitamin B_{12} for good maintenance and for the treatment for anemia as it instigates red blood cell formation. Cobalt has unique electrical, catalytic, magnetic and optical characteristics that makes it suitable for broad-ranging applications comprising, nanosensors, nanoelectronic gadgets and catalyst. It operates as the model system for the macroscopic magnetic response due to the low to medium crystal anisotropy permitting the influences of morphologies, sizes, internal crystal structures, and surface anisotropy to be recognized in one system (Faucon, Pourret, & Lange, 2021). Cobalt and its three metastable phases with various crystallographic structures, including the hexagonal closed packed, face centered cubic, and epsilon phases, has been considered as one of the most important ferromagnetic metals (Siavash Iravani & Varma, 2020).

Cobalt oxide is a recognized antiferromagnetic p-type multifunctional semiconductor with spinel crystal structure; the direct optical band gaps of Co_3O_4 NPs being about 1.48 and 2.19 eV, renders it as a suitable photocatalyst for the degradation of organic pollutants using visible light. Cobalt, in its oxide forms can be found in different spin states, including high, low and intermediate spin which imparts attractiveness to the physics of the Co_3O_4 from a fundamental standpoint besides spintronic applications (Raveau & Seikh, 2015). These NPs have numerous significant applications (Figure 6) in areas such as field effect transistor, storage of energy, catalysis, anode material in rechargeable Lion batteries, electrochromic sensors, solar cells and as a photocatalyst. Additionally, these NPs have antibacterial, anticancer, antioxidant, antifungal, and enzyme inhibition properties, because of their superior biomedical applications (Waris et al., 2021).

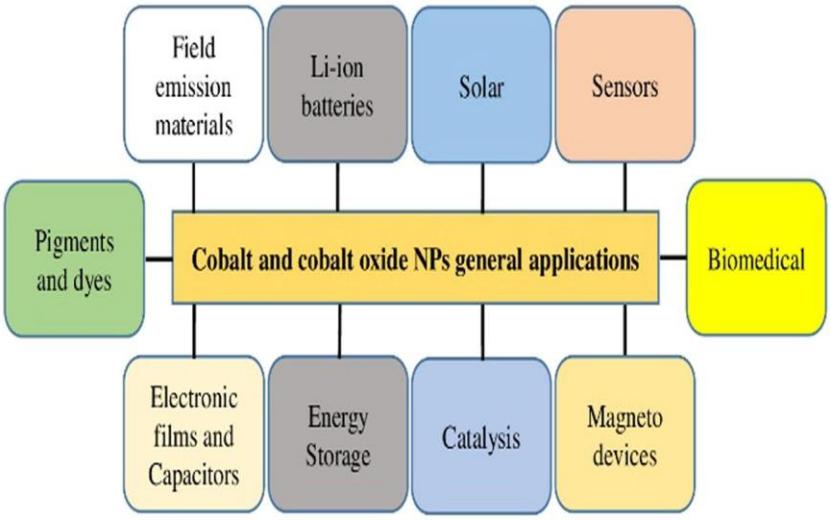

Figure 6: General applications of cobalt and cobalt oxide NPs (Waris et al., 2021)

2.3.3 Doping of Titanium Oxide Nanoparticles

Doping of TiO_2 has been an important approach in band gap engineering to change the optical response of semiconductor photocatalysts. The main objective of doping is to induce a bathochromic shift, i.e., a decrease of the band gap or introduction of intra-band gap states, which results in the absorption of more visible light. Doping may lead to photocatalytic systems that exhibit enhanced efficiency. It is desirable to maintain the integrity of the crystal structure of the photocatalyst while changing its electronic structure by doping. It is easier to replace Ti^{4+} in TiO_2 with a cation than to substitute O^{2-} with another anion because of the difference in the charge states and ionic radii (Basavarajappa et al., 2020). Nanomaterials show a higher tolerance to structural distortion than bulk materials due to their inherent lattice strain. As a result, the surface modification of TiO_2 nanoparticles appears to be more beneficial than the modification of bulk TiO_2.

2.3.3.1 Cobalt doped Titanium Oxide Nanoparticles

The large band gap metal oxide nanomaterials relatively causes difficulty in exciting and injecting the electrons, which leads to inefficient electron transportation and consequently poor electrical conductivity. One way to address this issue is to dope the semiconductor with metals to reduce the band gap; this enhances sunlight absorbance as well as the transportation of electrons in TiO_2 from photovoltaic and photocatalysis. Moreover, metal-doped TiO_2 slows down the recombination of photogenerated electron−hole pairs owing to the influence of the trap states and the electronic

structure of TiO_2.Among the various metallic dopants (e.g., Ni, Mg, Co, Fe, Ca, and Zn), Co has been considered as a suitable candidate for incorporation in TiO_2 structures as it considerably reduces the band gap energy of TiO_2, leading to increased light absorption. More importantly, doping with Co facilitates the generation of massive distortions and the accompanying defects resulting from the presence of Co atoms in TiO_2 lattices (Alothman et al., 2021).

Cobalt doped titanium oxide nanoparticles have been widely used as catalysts in various chemical reactions. The doping of cobalt into titanium oxide nanoparticles enhances their catalytic activity and selectivity. For instance, cobalt doped titanium oxide nanoparticles have been found to exhibit excellent catalytic activity in the degradation of organic pollutants such as phenol and methylene blue (Botsa et al., 2022; Lim & Hoffmann, 2020). The presence of cobalt atoms in the nanoparticle structure enhances the photocatalytic activity of titanium oxide nanoparticles, leading to higher efficiency in the degradation of organic pollutants. In addition, cobalt doped titanium oxide nanoparticles have been used as catalysts in the production of hydrogen gas through water splitting. The doping of cobalt into titanium oxide nanoparticles enhances their photocatalytic activity, leading to higher efficiency in the production of hydrogen gas (Sadanandam et al., 2013).

Cobalt doped titanium oxide nanoparticles have also been investigated for their potential use in energy storage devices. The doping of cobalt into titanium oxide nanoparticles improves their electronic conductivity and charge transfer properties, leading to higher efficiency in energy storage devices. For example, cobalt doped titanium oxide nanoparticles have been used as anode materials in lithium-ion batteries. The presence of cobalt atoms in the nanoparticle structure enhances the lithium-ion storage capacity of titanium oxide nanoparticles, leading to higher energy density and longer cycle life of the batteries. Moreover, cobalt doped titanium oxide nanoparticles have also been used as photoanodes in dye-sensitized solar cells. The doping of cobalt into titanium oxide nanoparticles enhances their light harvesting ability and electron transport properties, leading to higher efficiency in solar energy conversion (Kashale et al., 2019).

Cobalt doped titanium oxide nanoparticles have also shown potential in biomedical applications. The doping of cobalt into titanium oxide nanoparticles enhances their magnetic properties, making them suitable for magnetic resonance imaging (MRI). For instance, cobalt doped titanium oxide nanoparticles have been used as contrast agents for MRI imaging of cancer cells. The presence of cobalt atoms in the nanoparticle structure enhances the magnetic properties of titanium oxide

nanoparticles, leading to better contrast in MRI images. Moreover, cobalt doped titanium oxide nanoparticles have also been investigated for their potential use in drug delivery systems. The doping of cobalt into titanium oxide nanoparticles improves their biocompatibility and stability, making them suitable for drug delivery applications. For example, cobalt doped titanium oxide nanoparticles have been used as carriers for the delivery of anti-cancer drugs to cancer cells (Shenoy et al., 2022).

2.4 Wastewater treatment

Wastewater is used water that has been affected by domestic, industrial, and commercial use. Wastewater contains contaminants such as organic materials, microorganism, inorganic soluble compounds, and the use of toxic heavy metals. The chemical, biological, and physical characteristics of clean water are changed by this contaminants. The source of wastewater are mainly derived from various industries include agricultural sectors (Figure 7) (Matheyarasu et al., 2014). The water consumption from industrial is far less than agricultural uses but still much higher than household usage. A massive amount of water used from industries will generate a high volume of wastewater. Due to environmental pollution and human health concerns, all wastewaters must be treated before being discharged into the environment or reused (Selihin & Tay, 2022).

Wastewater contains large microorganisms, including viruses, bacteria, and protozoa and toxic substances, such as heavy metals, radionuclides, and trace elements. Wastewater is also one of the leading causes of waterborne diseases, including deadly conditions such as typhoid and cholera. Polluted water caused the death of more than 1.5 million children under the age of five in 2004 (Baek & An, 2011).

Wastewater treatment has become essential nowadays because of the toxic effects of pathogens and the hazards of wastewater pollution on humans, agriculture, and animals. Wastewater treatment at the personal and government level must be taken into account to protect the environment from pollution. The treatment of wastewater can involve physical, chemical, and biological procedures for water purification from various contaminants (Piaskowski, Świderska-Dąbrowska, & Zarzycki, 2018).

Figure 7: Sources of wastewater streams (Matheyarasu et al., 2014).

2.4.1 Wastewater treatment methods

Progressively developmental achievements are being accomplished in order to develop new strategies for wastewater treatment and fulfill the requirements of clean water (S. N. Ahmed & Haider, 2018). However, it has been challenging to treat discharged water containing pollutants thoroughly with available methods. Several techniques, such as physical, chemical, and biological processes that are considered effective enough for water treatment in many ways. Their selection depends on various factors like dye concentration, sewage composition, cost of the process, or the additional impurities present in wastewater (Wawrzkiewicz et al., 2019).

2.4.1.1 Physical method

Physical methods of wastewater treatment involve the removal of physical impurities from wastewater. These methods are typically used in the first stage of the treatment process, before chemical and biological treatment. The physical treatment of wastewater can be achieved through various methods, including screening, sedimentation, and filtration. These methods are used to remove different types of solid particles from the wastewater. Screening is the process of removing large objects and materials from wastewater, such as sticks, stones, and plastics. The wastewater is passed through a series of screens that trap these materials before they can cause damage to downstream equipment or interfere with the biological treatment process. Sedimentation is the process of allowing the wastewater to settle, so that heavier particles sink to the bottom of the tank,

while lighter particles float to the top. The settled particles, known as sludge, are removed from the bottom of the tank and sent to a separate treatment process. Filtration is the process of removing suspended solids from the wastewater by passing it through a filter medium. The filter medium can be sand, gravel, or other porous materials. The suspended solids are trapped in the filter media, while the filtered wastewater is collected and sent for further treatment (Safoniuk et al., 2004).

Mass transfer strategy is the base of the physical pollutant removal methods. It is more likely to be used due to its simplicity, flexibility, high efficiency, and pollutant recyclability (Wong et al., 2019). The fewer chemical requirement is another advantage of this approach. Physical treatment seems highly reliable than the other treatments because it does not depend on living organisms. Physical method of wastewater treatment include: adsorption (Liu et al., 2020), membrane filtration (Yang et al., 2020), and coagulation/flocculation (Yogalakshmi et al., 2020). Among physical methods, adsorption is usually considered a cost-effective and reliable method for wastewater treatment, and has been used by researchers in recent years because of its high efficiency and low operational cost.

Physical methods of wastewater treatment are effective in removing large particles and solids from the wastewater, but they are not always sufficient to meet discharge standards. Therefore, physical treatment is typically used in combination with chemical and biological treatment to achieve the desired level of treatment.

2.4.1.2 Chemical method

Chemical methods of wastewater treatment involve the use of chemicals to remove contaminants from the wastewater. Chemical treatment is typically used after physical treatment, as it can effectively remove dissolved contaminants and organic matter that may not be removed by physical treatment alone.

Several chemical oxidation processes are reported for a range of catalysis applications (Shafiq et al., 2022). However, the advanced oxidation process is considered an essential technique for wastewater treatment. AOPs is an acronym that indicates all methods used in wastewater treatment that have common principles in generating oxidizing species, such as hydroxyl radicals (•OH) (Sicardi, 2020). Oxidation may involve electrochemical oxidation, photo-electrochemical

oxidation and UV assisted Fenton's oxidation and ozonation. Generally, catalysts and pH play an essential role in the oxidation process.

The electrochemical advanced oxidation processes (EAOPs) has appeared as a promising technique for wastewater treatment (dye removal). EAOPs are environment friendly, as the electrons are inherently clean species, and no supplementary procedure is mandatory for removing dye sludge. Other benefits comprise high efficiency for the removal of pollutants, simple equipment, and easy handling. The main challenge that obstructs applications of EAOPs is increased energy costs with comparatively lower oxidation efficiencies. Attention has recently been paid to electrode materials' stabilities and catalytic activity improvement by the fabrication of different metal oxides on electrodes and doping (J. Wang et al., 2020).

In order to achieve high removal efficiencies and degradation of pollutants, advanced oxidation processes (AOPs), based on the active and strong oxidizing agents like hydroxyl (•OH) radicals, are desired to retain the level of pollution under legal limits. Among AOPs, •OH-based electrochemical processes are becoming increasingly importantIn the photo-electrocatalysis process, a chemical reaction occurs at the semiconductor anode to increase light efficiency in response to the electric current. A photoanode semiconductor is irradiated with solar light for removing a dye such as a methyl orange photo-electrochemically. •OH radicals, which are generated by water oxidation, mediate the oxidation of methyl orange. They are reactive enough to produce small molecules, aromatic ring-opening, and azo bond breakdown. When interest is just dye removal of wastewater, a high rate can be attained at high current and low primary concentrations, and the high yield can be achieved by operating at low concentrations and low current. Photo-electrocatalysis reduces the concentration of dyes and degrades them (Mais et al., 2020).

2.4.1.3 Biological method

Biological treatment is a critical stage in the process of wastewater treatment, used to remove organic matter and nutrients from the wastewater. Biological treatment involves the use of microorganisms to break down and convert the contaminants in the wastewater into harmless byproducts (Cepoi et al., 2016). There are two main types of biological treatment methods used for wastewater treatment: aerobic and anaerobic.

Microorganisms decompose or degrade organic colorants in biological treatment via aerobic or anaerobic cycle (Saxena & Bharagava, 2017). Microbes use organics as an energy source by degrading them. Biofilms are developed for the removal of contaminants from sewage water. The biological methods for the complete degradation of textile wastewater have benefits such as (a) eco-friendly, (b) cost-competitive, (c) less sludge production, (d) giving nonhazardous metabolites or complete mineralization, and (e) less consumption of water (higher concentration or less dilution requirement) compared with the physical/oxidation method. The efficiency of biological processes for degradation depends on the selected microbes' adaptability and enzymes' activity. Therefore, many microorganisms and enzymes have been isolated and tried for the degradation of several dyes. The isolation of potent microbes and their use of degradation is an interesting biological aspect of textile wastewater treatment. A wide range of microorganisms such as bacteria, fungi, and algae can degrade a wide variety of dyes present in the textile wastewater (Holkar et al., 2016).

In general, biological treatment is an essential step in the process of wastewater treatment, removing organic matter and nutrients that physical and chemical treatments may not be able to remove. The use of biological treatment is typically tailored to the specific contaminants present in the wastewater and the desired level of treatment required. The choice between aerobic and anaerobic treatment methods depends on the specific characteristics of the wastewater and the desired treatment outcomes.

2.5 Photocatalysis

The term photocatalysis is a combination of two words: photo related to photon and catalyst, which is substance altering the reaction rate in its presence. Therefore, photocatlyst are material that change the rate of chemical reaction on exposer to light. This phenomenon is known as photocatalysis. Photocatalysis include reaction that take place by utilizing of light and semiconductors. The substrate that absorbs light and acts as a catalyst for chemical reactions is known as a photocatalyst (Ameta et al., 2018). Photocatalysis is a surface phenomenon which commonly includes the following five mechanistic steps: (i) diffusion of reactants to the surface of the catalyst, (ii) adsorption of the reactants on the surface of the catalyst, (iii) reaction at the surface of the catalyst, (iv) desorption of the products from the surface of the catalyst, and (v) diffusion of the products from the surface of the catalyst.

Photocatalysis is currently being applied in wastewater treatment as two different types of applications: one is solar photocatalysis, and another is photocatalytic application system equipped with artificial UV-Visible light. Nanostructure semiconductor material are the most suitable photocatalyst because they have the most of the photogenerated electron and holes, which are available at the surface. Photocatalysis play an important role in the removal of organic and inorganic contaminants such as dyes, heavy metal ions, and microbes (Goutam et al., 2020).

A recent study by (Goutam et al., 2018) presents an excellent example of photocatalytic treatment/degradation of tannery wastewater using green synthesized TiO_2 NPs. Nanoparticle based photocatalytic treatment is a highly effective method for the degradation and detoxification of recalcitrant organic and inorganic pollutants from wastewater.

2.5.1 Photocatalytic mechanism of TiO_2 based photocatalysts

In photocatalysis, a photocatalyst is excited by light irradiation to induce oxidation and reduction. TiO_2, an n-type semiconductor, is used as a photocatalyst in many applications, such as defogging, air purification, water purification, disinfection, sterilization, and degradation (Subramanian et al., 2017). It has a large optical energy bandgap and hence requires excitation by low-wavelength light (<400 nm) to participate in photocatalysis (Xu et al., 2018). The schematic representation of photocatalytic degradation processes is shown in Figure 8. When UV light hits a TiO_2 catalyst, photogenerated e^-/h^+ pairs are created between its VB and CB. These pairs subsequently undergo recombination and trapping (Soman et al., 2018). Such photo-induced species are formed according to the reaction sequence given below, which includes the photoexcitation of TiO_2 (Eq. (1)), trapping of electron charge-carriers (Eq. (2)), trapping of hole charge carriers (h^+) (Eq. (3)), and recombination of photogenerated carriers (electron and hole pairs) on the surface of the semiconductor (Eq. (4)).

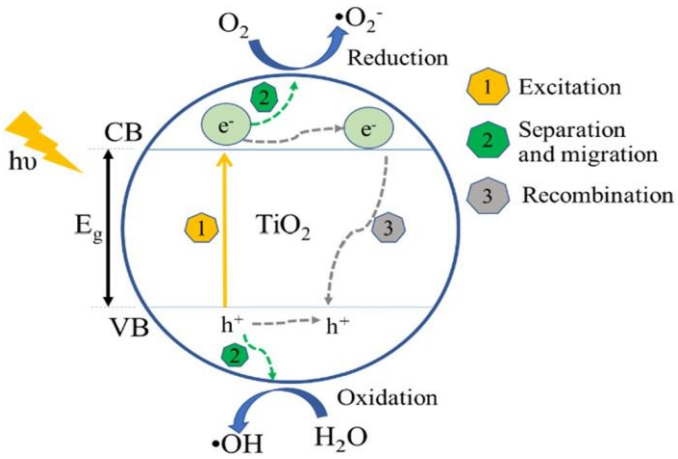

Figure 8: Excitation processes in TiO_2 under light irradiation (VB: valence band; CB: conduction band) (He, Kumar, Khan, & Lo, 2021)

$TiO_2 + h\nu \rightarrow e^- + h^+$ (1)

$e^-(CB) \rightarrow e^-(trapping)$ (2)

$h^+(VB) \rightarrow h^+(trapping)$ (3)

$e^-(trapping) + h^+(trap\ ing) \rightarrow heat$ (4)

Aqueous adsorbed oxygen trapped photo-induced electrons in the CB and participated in a reduction reaction to form $O_2^{\bullet}$ (Eq. (5)). $O_2^{\bullet}$ reacted with protonated H^+ ions (Eq. (6)) generated by the ionization of water (Eq. (7)). Excited electrons are trapped by $HOO^{\bullet}$ to yield HOO^- (Eq. (8)) and subsequently undergo protonation to produce hydrogen peroxide (H_2O_2) (Eq. (9)).OH^- radicals are produced by the decomposition of H_2O_2 (Eq. (10)). At the same time, photo-induced h^+ in the VB diffuse the catalyst surface and react with adsorbed water molecules to produce more OH^- (Eq. (11)).

$(O_2) + e^- \rightarrow O_2^{\bullet}$ (5)

$O_2^{\bullet} + H^+ \rightarrow HOO^{\bullet}$ (6)

$H_2O \rightarrow OH^- + H^+$ (7)

$HOO^{\bullet} + e^- \rightarrow HO_2^-$ (8)

$HOO^- + H^+ \rightarrow H_2O_2$ (9)

$H_2O_2 + e^- \rightarrow OH^- + OH^{\bullet}$ (10)

$H_2O + h^+ \rightarrow H^+ + OH^\bullet$ (11)

$OH^\bullet + O_2^\bullet + h^+ + e^- + \text{organic molecules} \rightarrow \text{byproducts}$

Different organic molecules are transformed, degraded, deactivated, or decomposed by $^\bullet OH$, h^+, e^- and other oxidizing agents to produce by-products.

2.5.2 Techniques for enhancing photocatalytic activity of TiO_2

TiO_2 photocatalyst has a high band gap value which results in low conversion efficiency under visible light. This implies that TiO_2 may only be stimulated under the UV radiation. Thus, it becomes essential to develop a TiO_2 photocatalyst which can be stimulated by visible light for greater feasibility of its applications under minimal conditions. As mentioned earlier, the recombination of the charge carriers also reduces the photo-efficiency of the photocatalyst. Modifications are thus required to ensure a lower rate of recombination for TiO_2 to function optimally. Several strategies were employed for modification, however doping of TiO_2 with either metals or nonmetals remains one the most common methods used for its sensitization to visible light and reduction in the rate of recombination of charge carriers (Sakhare et al., 2014).

2.5.2.1 Metallic Doping

Cations, such as rare earth metals, noble metals, poor metals, and transition metals have been used to dope TiO_2. Metallic doping to TiO_2 results in widening of the light absorption range which is accompanied by augmentation in the redox potential of the photo-generated radicals and also in the inhibition of recombination of the generated charge carriers. However, the nature, the concentration of the dopant, the photocorrosion process, and the induced space charge layer length alter the surface property of the materials and influence the photocatalaytic property accordingly. Although, several studies depict the improvement of visible light absorption capabilities of the metal-doped TiO_2 (Zhu et al., 2006) (Ghicov, Schmidt, Kunze, & Schmuki, 2007), it is important to mention that the increase in the visible light absorption is not the only sole factor to promote the photoactivity of TiO_2. In fact, during cation implantation, a specific amount of defects might be created which act as centers of recombination, which is the driving force underlying the reduction in the photocatalaytic activity. This undesirable effect might be avoided by the reannealing of the doped TiO_2. Moreover, doping of TiO_2 with cations displaying either higher or lower oxidation states promotes the rise in the electrical conductivity. When TiO_2 is doped with metallic cations

having lower oxidation state electron neutrality may be achieved by removal of electrons from the valence band. The leaping of electrons generates holes in the valence band of the system, which results in the elevation in the electrical conductivity. In comparison, when TiO_2 is doped with metallic cations possessing higher oxidation states, the electron neutrality in the system might be achieved by electron addition into the already empty conduction band. These electrons that are transferred into the conduction band result in the augmentation of the electrical conductivity (Dunnill, Kafizas, & Parkin, 2012).

2.5.2.2 Non-metallic Doping

Considerable efforts have been made to extend the photoactivity of TiO_2 based systems into the visible light region for the efficient utilization of solar energy. Nonmetal doping is an alternative for improving the visible light response of TiO_2, and extensive research work has been done on synthesis of N-doped, S-doped, F-doped, and C doped TiO_2. The doping with nonmetal could narrow down the band gap by modifying the electronic structure around the conduction band edge of TiO_2, by incorporating anion into the crystal lattice of TiO_2. This might drive better photocatalytic performance under visible light. Recently, many researchers paid much attention to nitrogen-doped TiO_2, which can be produced using different techniques, such as hydrolytic process mechano chemical technique. Nitrogen can be easily introduced in the TiO_2 structure, due to its comparable atomic size with oxygen, small ionization energy and high stability (Patil et al., 2019). Figure 9 here shows the electron transfer mechanism of N - doped anatase - rutile heterojunction.

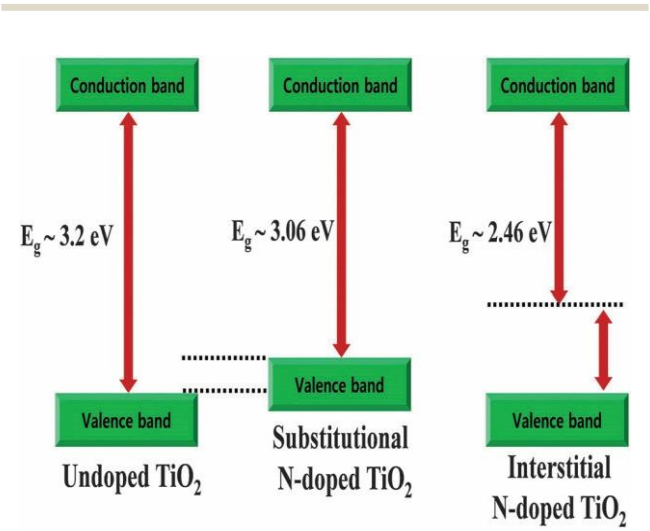

Figure 9: Schematic diagram showing the valence and conduction bands of undoped and N-doped TiO_2 (Ansari et al., 2016)

3. Materials and methods

3.1 Chemicals and materials

The analytical grade chemicals that were used for the synthesis of TiO_2 and Co-doped TiO_2 nanoparticles includes Titanium tetra-butoxide (TTBO) ($Ti(C_4H_9O)_4$, Sigma Aldrich, 98%), sodium hydroxide (NaOH, Labo chemie;98%), cobalt nitrate hexahydrate ($Co(NO_3)_2$. $6H_2O$ Unichem;99%), Methylene blue (Unichem), distilled water (DW), and absolute ethanol (Labo chemie;99.8%). For anti-bacterial activity analysis, nutrient broth (Sirchem) and Mueller Hinton agar (Sirchem) were used for medium preparation. Other experimental apparatus and setups such as, volumetric glass, Erlenmeyer flask, beakers, test tube, pH meter, paper disc, nutrient agar disc, magnetic stirrer, hot plate, digital balance, dropper, centrifuge, muffle furnace, refrigerator were used.

3.2 Preparation of plant extract

The *Millettia ferruginea* plant was collected from Chiko Maya Kebele of Aleta Wondo Zone; Sidama regional state, Ethiopia. The leaves of the plant were washed with tape water and then with DW, and subsequently cut into small pieces after air drying. The dried leaves of the plant were crushed to powder using mortar and pestle. Next, 15 g of the powdered plant was added to a beaker containing 400 milliliters of absolute ethanol. The mixture was heated at 40℃ for 40 min and the resulting supernatant was filtered using a Whatman filter paper. The filtrate was then stored in refrigerator at 4℃ for further use in the synthesis of nanoparticles (Uddin et al., 2021).

3.3 Synthesis of undoped TiO_2 NPs

To synthesized TiO_2 NPs, a mixture of 0.2 M TTBO and leaf extract of *Millettia ferruginea* were used in various volume ratios: 1: 1 (75 mL of precursor salt and 75 mL of leaf extract), 2: 1 (100 mL of precursor salt and 50 mL of leaf extract), and 1: 2 (50 mL of precursor salt and 100 mL of leaf extract). The resulting NPs were labeled as TiO_2 (1: 1), TiO_2 (2: 1), and TiO_2 (1: 2). The solution of different volume ratios were stirred for approximately five hours at room temperature, without heating. Sodium hydroxide solution (1M) was added to a solution as a precipitating agent to bring the pH to 10. The resulting precipitates were then centrifuge at 1000 rpm for 15 min and washed four times sequentially with distilled water and absolute ethanol. Following the final centrifugation, the resulting TiO_2 NPs were collected in a crucible and dried overnight in a drying

oven at 100℃ (Santhoshkumar et al., 2014). The synthesized TiO_2 NPs were calcined at 500℃ (from thermal analysis) for four hours. Figure 10 shows the synthesis procedure of undoped TiO_2 NPs using ethanolic extract of *Millettia ferruginea.*

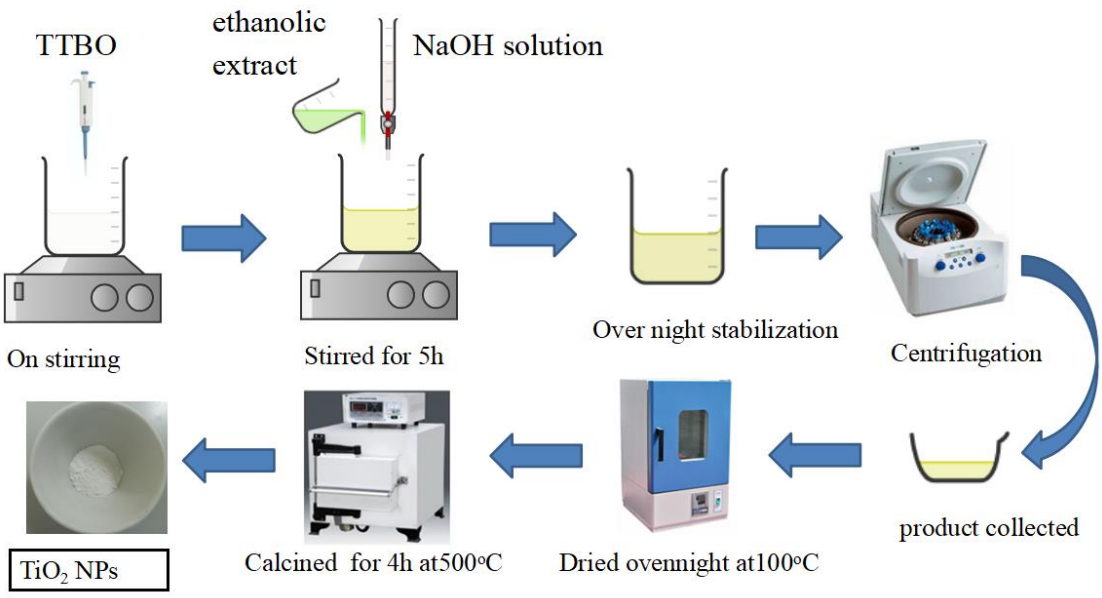

Figure 10: schematic representation for the synthesis procedure of undoped TiO_2 NPs using ethanolic extract of *Millettia ferruginea.*

3.4 Synthesis of Co-doped TiO_2 NPs

The Co-doped TiO_2 NPs were synthesized through a co-precipitation method at room temperature using TTBO and cobalt nitrate hexahydrate ($Co(NO_3)_2 \cdot 6H_2O$) as precursor materials. For the typical synthesis, 100 mL TTBO solution placed into three different beakers and An appropriate amount of cobalt nitrate hexahydrate ($Co(NO_3)_2 \cdot 6H_2O$) were added to this solution to produce 2 wt%, 4 wt %, and 6 wt % Co proportion in each beakers. Then 50 mL leaf extract of *Millettia ferruginea* were added to each beakers as stabilizing and reducing agent. The pH of the solution was adjusted to pH 10 by drop wise addition of an aqueous solution of NaOH (1M). The resulting precipitates were washed with distilled water and ethanol four times. The precipitate were dried overnight in a drying oven at 100℃ and calcined at 500℃ for four hours (Kashale et al., 2019). Figure 11 shows the synthesis procedure of Co-doped TiO_2 NPs using ethanolic extract of *Millettia ferruginea.*

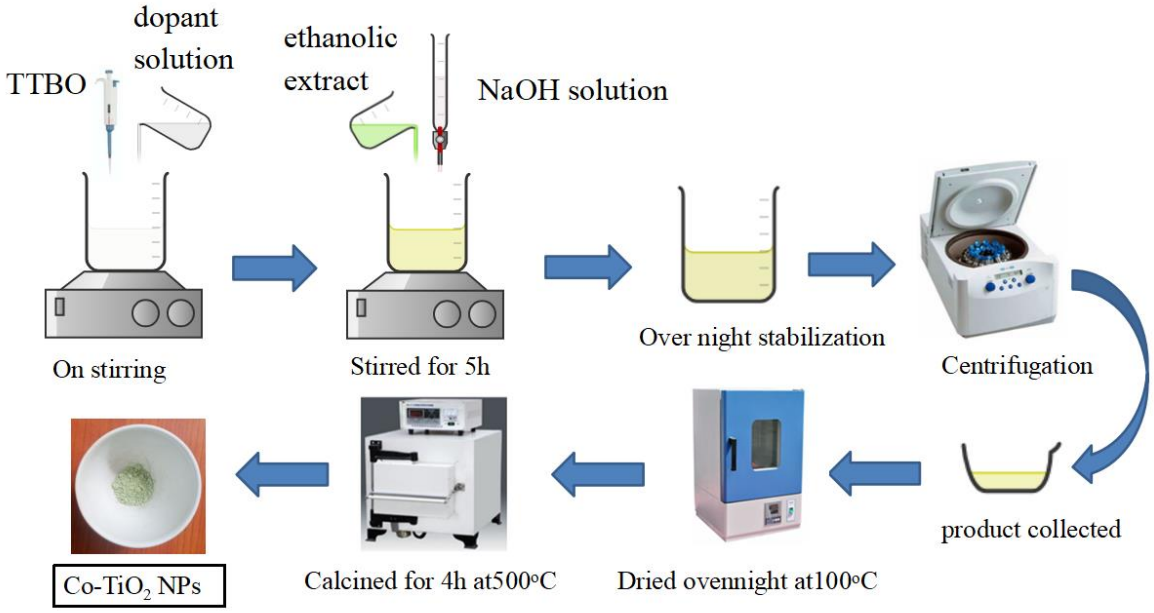

Figure 11: schematic representation for the synthesis procedure of Co-doped TiO_2 NPs using ethanolic extract of *Millettia ferruginea.*

3.5 Characterization

The thermal stability of the synthesized undoped and Co-doped TiO_2 NPs were analyzed by means of thermogravimetric and differential thermal analysis (TGA/DTA) apparatus (DTG-60H Shimadzu Co., South Korea). The crystallinity of the synthesized nanostructures were evaluated by using an X-ray diffractometer (XRD-700 Shimadzu Co., Japan, λCuK1 = 0.15406 nm, tube voltage 40 kV, current 30 mA), and the morphology of the synthesized nanostructures were studied via scanning electron microscopy (SEM, Hitach S4800, Japan). The optical properties of the synthesized nanostructures were studied with a UV-Vis diffuse reflectance spectrometer (UV-3600 Shimadzu Co., Japan). Fourier transform infrared (FTIR) spectra were also used to confirm the formation of NPs and the presence of any functional group (Jasco, FT/IR-6600, Japan).

3.6 Photocatalytic activity

The photocatalytic activity of the synthesized samples was evaluated by the degradation of an aqueous solution of MB. The reaction was carried out in a discontinuous mechanical stirring photoreactor with 150 W halogen lamp irradiation. For the effective degradation of MB dye, 20 mg of the catalyst was added in to 100 mL of 10 ppm solution of MB under constant stirring. The

solution was stirred continuously for 30 min before irradiation in a dark condition to reach an adsorption-desorption equilibrium between MB and catalyst. Then, the light source was positioned on top of the solutions and the sample was irradiated under continuous stirring. A (5-10) mL of the solution under irradiation was taken periodically every 20 min and subjected to centrifugation to separate out the catalyst. The concentration of MB in each portions of solution taken was estimated from the absorbance at 664 nm using a UV–Visible spectrophotometer (UV-3600 Shimadzu Co., Japan). Finally, the photocatalytic degradation efficiency of the samples was calculated using the following equation (equ.12) (Cahino et al., 2019).

$$\text{Photo-degradation rate} = \left(\frac{A0-At}{A0}\right) \times 100 \qquad (12)$$

Here A_0 is the initial absorbance of dye solution and A_t is the dye solution absorbance at a certain reaction time. All Absorbance values were obtained by the wavelength of maximum absorption (λ_{max} = 664 nm) for MB in the absorption spectrum.

3.6.1 Effect of initial dye concentration

The effect of initial dye concentrations on the photocatalytic degradation efficiency of the synthesized catalyst against MB was studied by taking 100 mL of 10, 15, and 20 ppm solutions of MB and 20 mg of catalyst. After 80 min irradiation time, the catalyst was separated by centrifugation and the concentration of MB remaining in the solution for each concentration was estimated by measuring its absorbance at 664 nm using a UV–Visible spectrophotometer (UV-3600 Shimadzu Co., Japan). All other parameters were kept constant. Finally, the percent degradation of MB dye was determined from the initial and final concentration of MB for each concentration (Yadav, Tyagi, & Yadav, 2011).

3.6.2 Effect of pH

The effect of pH was studied at the pH values of 5, 7 and 9 using 100 mL of 10 ppm MB solution and 20 mg of synthesized catalyst at room temperature. The pH values of the solution was adjusted by the drop wise addition of 0.1 M HCl and 0.1 M NaOH solutions. After 80 min irradiation time, the catalyst was separated by centrifugation and the concentration of MB remaining in each solution was estimated by measuring its absorbance at 664 nm using a UV–Visible spectrophotometer (UV-3600 Shimadzu Co., Japan). Finally, the percent degradation of MB dye was determined from the initial and final concentration of MB in each solution (Guesh et al., 2016).

3.6.3 Effect of catalyst dosage

The effect of catalyst dose on MB degradation was investigated using a catalyst concentrations of 10 mg, 20 mg, 30 mg, and 50 mg. The amount of MB used in each dose of catalyst was 100 mL of 10 ppm. After 80 min irradiation time, the catalyst was separated from the solution by centrifugation. The concentration of MB remaining in the suspension of each solution was determined from the absorbance measurement obtained from UV-Vis spectrophotometer (UV-3600 Shimadzu Co., Japan) at a wave length of 664 nm. Then, the percent degradation of MB dye was determined from the initial and final concentration of MB (Cahino et al., 2019).

3.6.4 Kinetic studies

Kinetic studies of the photocatalytic degradation of MB were analyzed using pseudo first order and pseudo second order kinetics model. In first order kinetics reaction, the rate constant k (min^{-1}) was determined from the slope of the natural logarithm of the concentration versus time plot as expressed in equation 13. On the other hand, in second order kinetics reactions the rate constant k ($M^{-1}\,min^{-1}$) was determined from the slope of the inverse of concentration versus time plot equation 14 (Alkaykh, Mbarek, & Ali-Shattle, 2020).

$$\ln\left(\frac{Ct}{Co}\right) = -kt \qquad 13$$

$$\frac{1}{Ct} = \frac{1}{Co} + kt \qquad 14$$

where C_0 is the initial concentration of the MB, Ct is the final concentration after visible light irradiation and k is the rate constant. The temporal changes of MB concentration (C/C_0) were proportional to maximum absorbance (A/A_0), λ = 664 nm).

3.7 Antibacterial studies

The antibacterial activity of the synthesized NPs was evaluated against Gram-positive and Gram-negative bacteria using the standard disc diffusion method (Humphries et al., 2018). The bacterial strains that were used for the antibacterial study were *Escherichia coli, Pseudomonas aeruginosa, Staphylococcus aureus, and Streptococcus pyogenes*. The first step involved the preparation of Mueller-Hinton agar solution, which was subsequently sterilized. Following sterilization, the agar solution was poured in to previously sterilized petri dishes with in a laminar flow chamber and allowed to solidify. The inoculum was spread uniformly onto each petri dishes using sterile cotton

swab. Next, sterilized discs were added in to different solutions of synthesized NPs along with different concentration (50, 25, 12.5 and 6.25 mg/mL). The discs containing the NPs were taken out of the solution and placed to each solidified Petri dishes. Negative and positive controls were also used, where Dimethylsulfoxide (DMSO) was used as the negative control, and ciprofloxacin was used as the positive control. The Petri dishes were then left at room temperature for 30 min for proper diffusion and incubated at 37℃ for 24 hours for each bacterium. After 24 hours, the plates were taken out from the incubator, and the inhibition zones were measured using a millimeter ruler.

4. Results and discussion

4.1 Thermal analysis

Thermogravimetric and differential thermal analyses were used to examine the thermal behavior of the synthesized TiO_2 NPs. This study was done to determine the calcination temperature of the synthesized samples during synthesis process. The TGA/DTA graphs of TiO_2 NPs synthesized by *Millettia ferruginea* leaf extract were shown in Figure 12. TGA curve displays weight loss of the synthesized sample while DTA curve shows the energy gain or loss throughout the process. Below 150℃, the percent weight loss observed could be due to the removal of physically and chemically entrapped water molecules. Between 150 and 465℃ , the percent weight loss also happened because of the breaking down of organic molecules (Bekele et al., 2020). The overall weight loss percentage calculated to be 11.2%. Furthermore, the endothermic peak on the DTA curve at 113℃ , corresponds to the release of water that has been adsorbed on the surface of particles. The exothermic peak at about 350℃, could be due to combustion of organic substances (Dakroury et al., 2022). As it is evident from the results of the TGA/DTA investigation, the synthesized TiO_2 NPs are thermally stable for temperature ranges higher than 500℃.

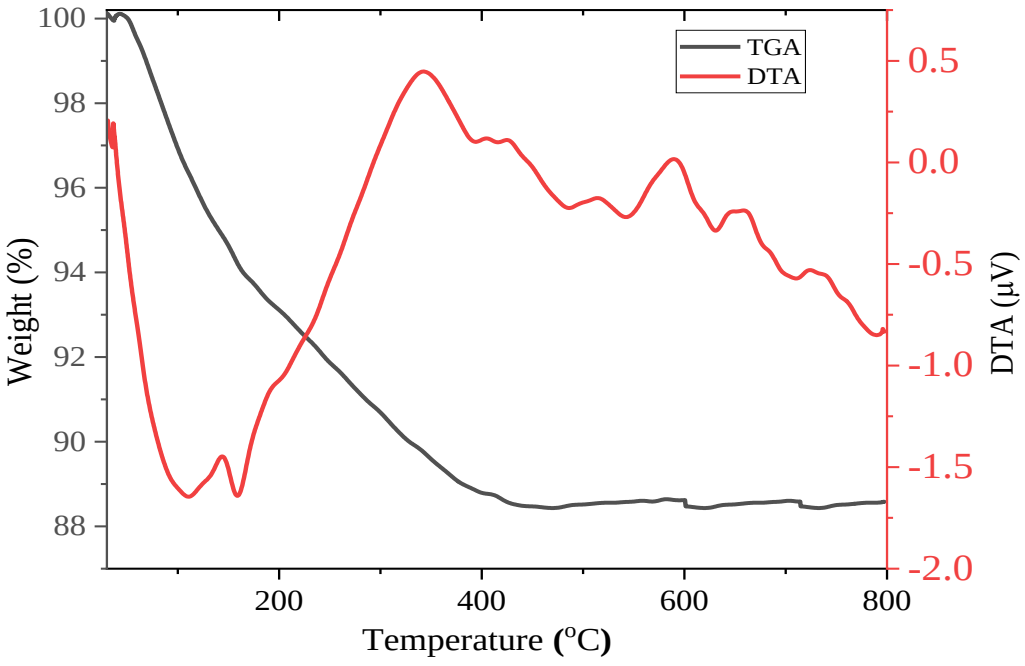

Figure 12. TGA/DTA of TiO_2 NPs synthesized by *Millettia ferruginea* leaf extract.

4.2 XRD analysis

The crystalline structure of the as synthesized undoped and Co-doped TiO_2 NPs were characterized by XRD. Figure 13 is showing the XRD patterns of the synthesized undoped and Co-doped TiO_2 NPs. As it can be observed from Figure 13, XRD pattern shows diffraction peak at 2θ valus of 25.3°, 37.8°, 48°, 53.9°, 55°, 62.7°, 68.8°, 70.2°, and 75.1°, with their corresponding miller indices of (101), (004), (200), (105), (211), (204), (116), (220) and (215) respectively. The XRD of undoped and Co-doped TiO_2 NPs fits with standard XRD pattern of tetragonal anatase phase of TiO_2 (JCPDS card no. 21-1272). There are no indications of the rutile and brookite phases, as well as pure cobalt and cobalt oxide. Not having these signatures in the XRD confirms the formation of single anatase phase TiO_2 NPs. As dopant concentration increased the peak brooding is observed, but with increasing dopant concentration up to 6 wt % Co no additional significant peak is seen (Khurana, Pandey, & Chudasama, 2015).

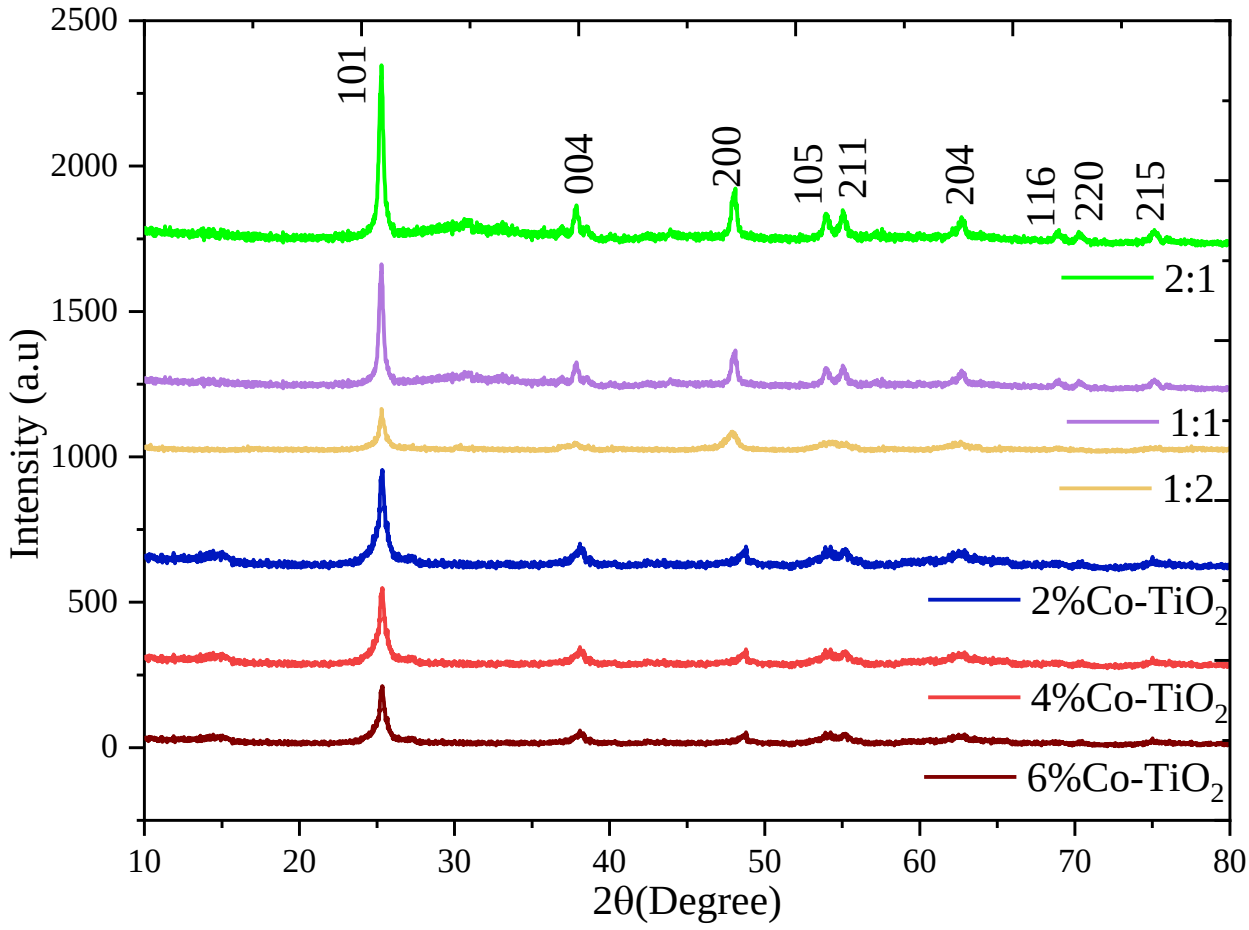

Figure 13: XRD patterns of undoped and with 2%, 4%, and 6% Co-doped TiO_2 NPs.

The average crystallite size of undoped and Co-doped TiO_2 NPs were assessed from the three most intense peak (101), (004), and (200) by using the Scherrer formula, the Eq. (15)

$$D = \frac{K\lambda}{\beta\cos\theta} \quad (15)$$

where K is Scherrer's constant, which is 0.9, λ is the wavelength of the X-ray radiation which is 0.15406 nm, β is peak width at half maximum, and θ is Bragg's angle. Hence, the average crystallite size of the all samples were calculated and reported in Table 1.

As it can be seen from table 1, the average crystallite size of undoped TiO_2 NPs synthesized using 2:1 ratio is smaller than that of 1:1 and 1:2 ratio. This could be due to the use of proper extract volume ratio that can help to maintain the stability of the TiO_2 NPs. In the case of doped sample, the average crystallite size of Co-doped TiO_2 NPs decrease with increasing dopant concentration due to the introduction of strain. When Co atoms are introduced into the TiO_2 lattice, they can cause lattice distortion as a result of ionic radii difference. These lattice distortions can lead to an increase in internal strain energy within the material. The strain energy rises along with the Co dopant concentration, which can result in a decrease in the average crystalline size of the material (Arda et al., 2015)

The lattice parameters a and b of the tetragonal structure of Co-doped TiO_2 NPs shows no much deviation from that of the undoped TiO_2 NPs with increasing concentration of Co (Table 1). In contrary to this, the lattice parameter of Co-doped TiO_2 NPs with long axis in c direction is showing slight increase compared to the undoped sample. A further increase in cobalt content over 2 wt % cause an increase in lattice constant c. These small variations in the lattice constant 'c' might be due to the difference in the ionic radii of Ti^{4+} and Co^{2+} ions (Mansour, Farha, & Kotkata, 2019).

Table 1: crystallite size (D) and Lattice constants (a, b, c) obtained from XRD analysis for undoped TiO_2 and Co-doped TiO_2 NPs.

Sample	Average crystallite size	Lattice parameter	
		a = b (A°)	c (A°)
2:1	16.8	3.7862	9.4988
1:1	18	3.7855	9.4957
1:2	23.3	3.7834	9.4925
2%	16	3.7829	9.4896
4%	15.6	3.7867	9.5011
6%	15.1	3.7872	9.5048

4.3 UV-Vis DRS analysis

The Optical characteristics of the synthesized samples were evaluated by utilizing UV-Vis DRS, and Tauc plots were generated through standard procedure and mathematical computations as shown in Figure 14. The band gap energy of both the undoped and Co-doped TiO_2 NPs was then determined using the Tauc equation (Tauc, Grigorovici, & Vancu, 1966).

$$(F(R) \cdot h\upsilon)^n = A \cdot (h\upsilon - E_g) \quad (16)$$

where F(R) is the percentage of reflected light, h is Planck's constant, ν is incident light frequency, E_g is the bandgap energy, A is a proportionality constant and n is the power index that is related to the characteristics transition in a semiconductor (n = 2). The optical bandgap energy of the NPs was estimated by plotting the $(F(R)\cdot h\nu)^n$ versus the photon energy (hυ) and extrapolating the linear region of the curve to the energy axis.

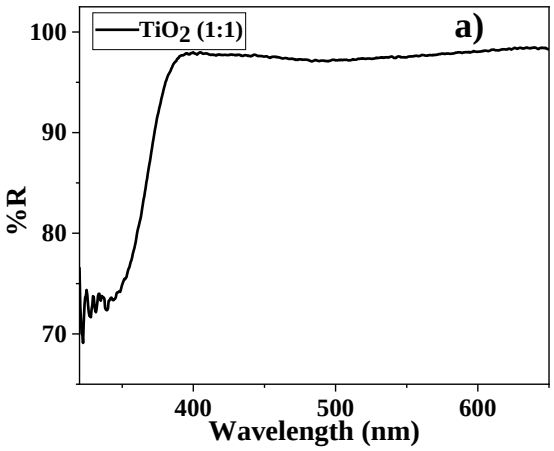
TiO2 (1:1)
a)
%R
Wavelength (nm)

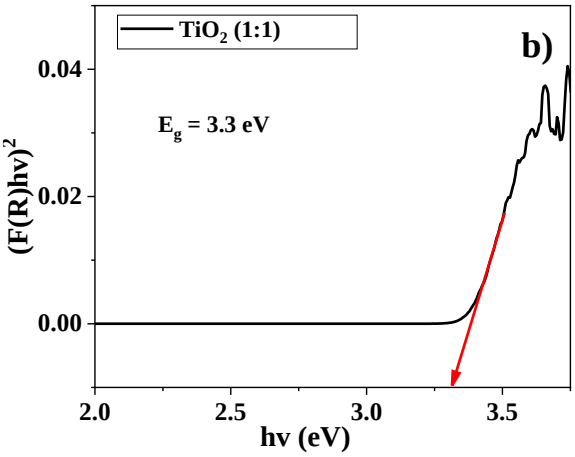
TiO2 (1:1)
b)
Eg = 3.3 eV
(F(R)hv)2
hv (eV)

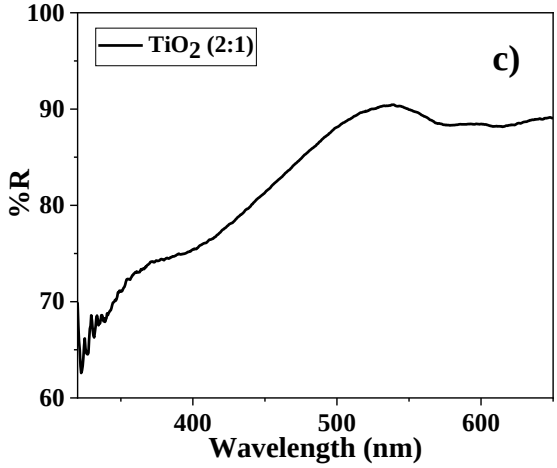
TiO2 (2:1)
c)
%R
Wavelength (nm)

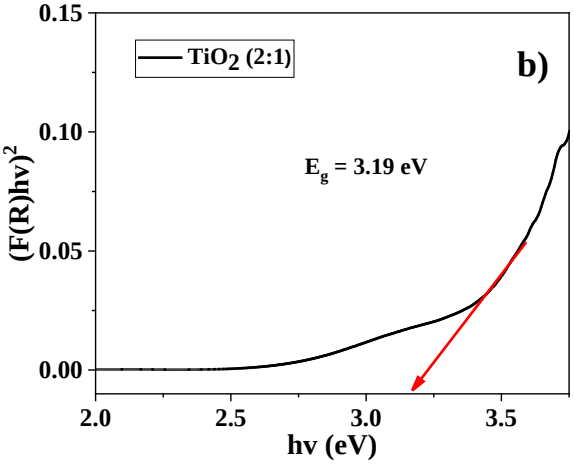
TiO2 (2:1)
b)
Eg = 3.19 eV
(F(R)hv)2
hv (eV)

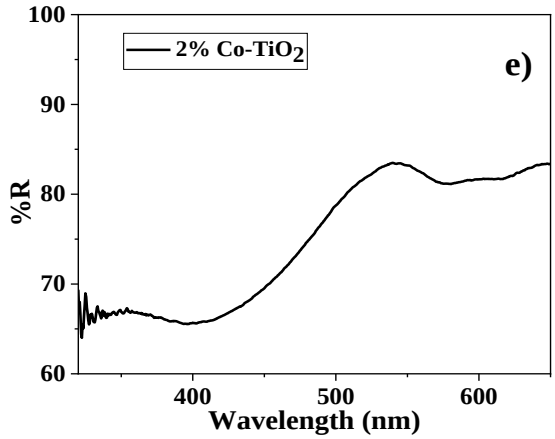
2% Co-TiO2
e)
%R
Wavelength (nm)

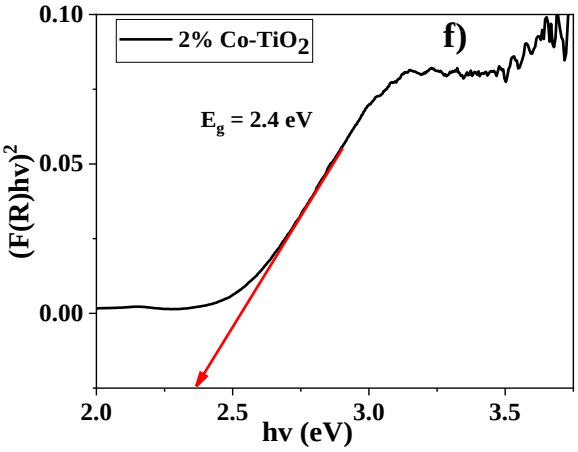
2% Co-TiO2
f)
Eg = 2.4 eV
(F(R)hv)2
hv (eV)

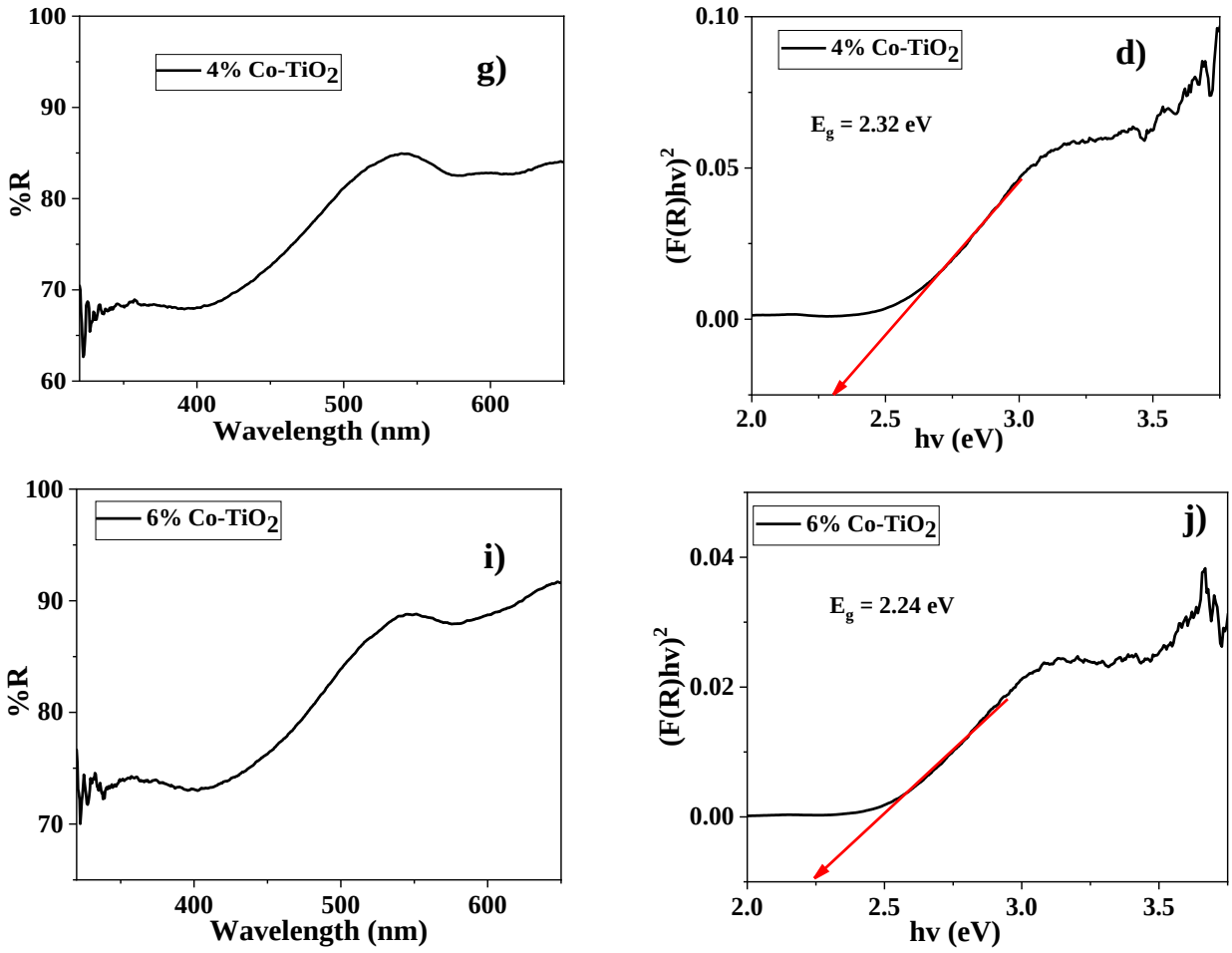

Figure 14: UV–Vis DRS spectra of TiO_2 (1: 1) (a), TiO_2 (2: 1) (c), 2%Co-TiO_2 (e), 4%Co-TiO_2 (g), and 6%Co- TiO_2 (i); and Tauc plots for bandgap energy estimation of TiO_2 (1: 1) (b), TiO_2 (2: 1) (d), 2%Co-TiO_2 (f), 4%Co-TiO_2 (h), and 6%Co-TiO_2 (j).

Figure 14(b and d) shows energy band gap of undoped TiO_2 NPs obtained from Tauc plots. The experimental energy band gap of TiO_2 (1: 1) and TiO_2 (2: 1) synthesized by *Millettia ferruginea* leaf extract were 3.3 eV and 3.19 eV respectively. The energy was found to be decreased with decreasing extract volume ratio. The result is in good agreement with the average crystalline sizes obtained from XRD. Therefore, TiO_2 (2: 1) ratio was used as host material for cobalt doping.

Figure 14(e, g, and i) shows the influence of Co-doping on the optical properties of TiO_2 NPs. Co-doped TiO_2 NPs exhibit a reflection band in the visible range above 400 nm. Furthermore, a smaller bandgap was proven by the doped samples' shifting of their reflection edge towards higher wavelengths. This red shift in Co-doped TiO_2 NPs can be explained due to sp-d exchange

interactions between the band electrons and the localized d electrons of the Co^{2+} ions substituting Ti^{4+} cations. The interactions of the p-d and s-d exchange lead to upward transformation of the valence band edge and downward transition of the conduction band edge which result in a reduction of band gap. The energy band gap of Co-doped TiO_2 NPs, as determined by Tauc plots, is shown in Figure 14(f, h, and j). Estimated band gap of 2%Co-TiO_2, 4%Co-TiO_2, and 6%Co-TiO_2 NPs were 2.4 eV, 2.32 eV and 2.24 eV respectively. As wavelength was increased, band gap shifted towards small values that's mean photo catalytic activity can be increased (Akbar et al., 2020; Koli et al., 2020).

4.4 FTIR analysis

The FTIR spectra of undoped TiO_2, and Co-doped TiO_2 NPs are shown in Figure 15. The absorption peaks at about 3408 and 1629 cm^{-1} are related to stretching vibration of surface hydroxyl groups and H-O-H bending vibration of adsorbed water molecules, respectively (Adyani & Ghorbani, 2018). The weak absorption band at around 2337 cm^{-1}, can be related to the absorption of CO_2 from the atmosphere. The peaks at 2,915 and 2,850 cm^{-1} are assigned to C–H stretching vibrations of alkane groups. The alkane and carboxylic groups specified by different bands are arise from TTBO (precursor material) (Mugundan et al., 2015). A small absorption peaks between 400 and 460 $cm^{-1}$are attributed to Ti-O-Ti vibrations. A shift of this band position to a lower wave number was observed for Co-doped TiO_2 NPs, indicating the presence of Co−O bonds due to the replacement of Co^{2+}at the Ti^{4+} sites in the TiO_2 lattice (T. M. H. Nguyen & Bark, 2020).

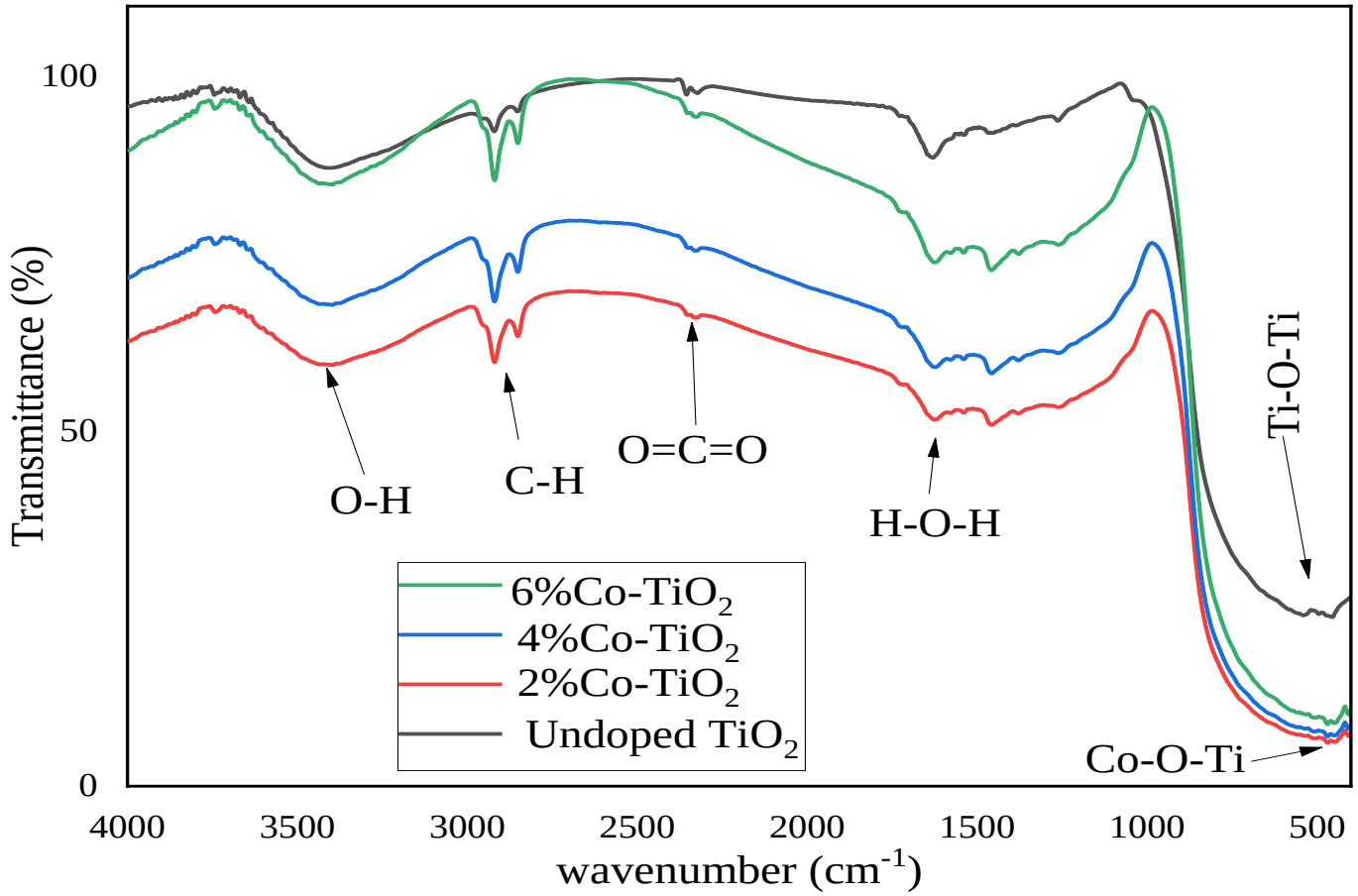

Figure 15: FTIR spectra of undoped TiO_2 and Co-doped TiO_2 NPs.

4.5 SEM analysis

SEM analysis was performed to determine the surface morphology of undoped TiO_2 and Co-doped TiO_2 NPs using scanning electron microscopy (SEM, Hitach S4800, Japan) and results were shown in figure 16. As indicated from figure 16(a-d), the surface morphology of all samples was an aggregates of spherical particles (Sundrarajan et al., 2017). At lower Co doping (2 wt %) the surface looks slightly porous. With increasing in Co content doped in TiO_2, the uniform particle agglomeration was increased and rough particle surface appeared. The photocatalytic activity of the synthesized material could be related to the surface roughness. The particle size was found to be decreased with increasing amount of Co ions in the host TiO_2. Whereas particle agglomeration was enhanced due to the incorporation of Co into TiO_2 structure. This agglomeration with decrease in particle size could be resulted from the higher surface energy exhibited by the small particles. The higher surface energy of particles promotes the surface to surface recombination of particles. Additionally, due to calcination and increased agglomeration between metals and TiO_2 particles,

the particle size was small, which further suggests that metal doping can suppress the growth of TiO_2 particles (Biru, Qaderi, Mamat, & Jalil, 2021; Nankya & Kim, 2016).

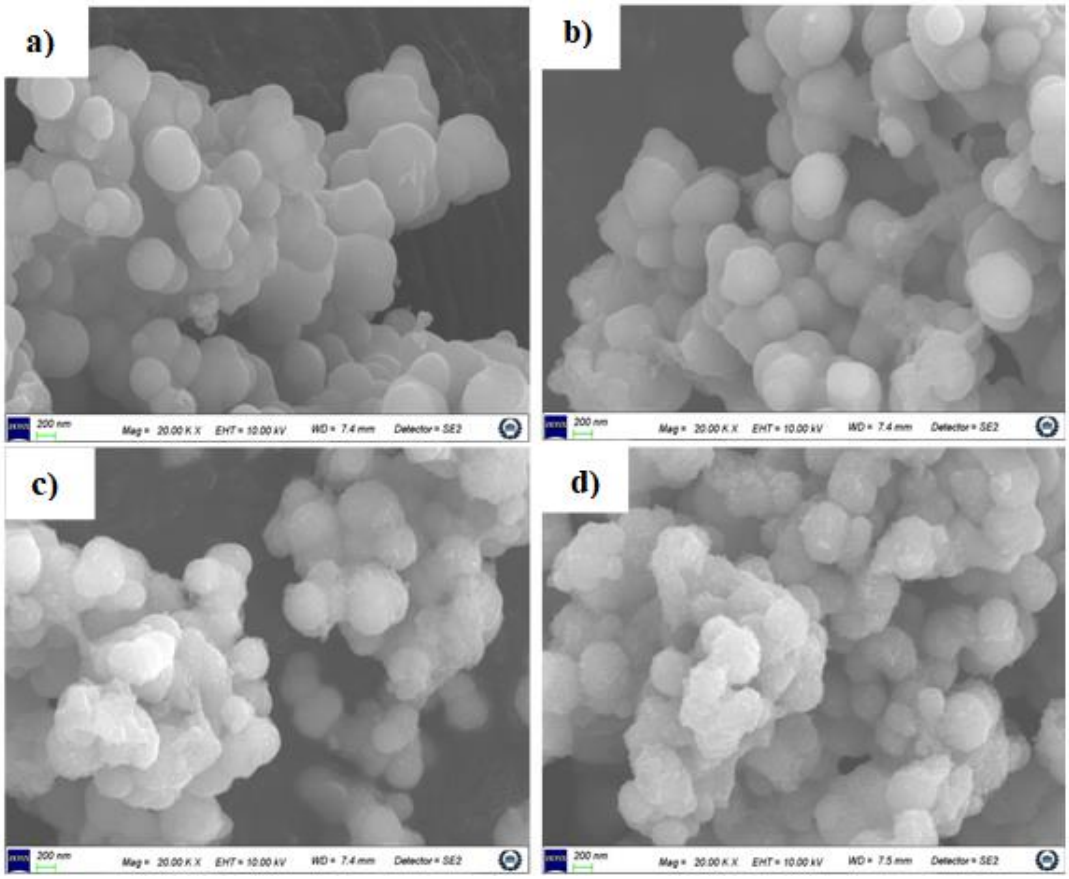

Figure 16: SEM image of undoped TiO_2 (a), 2%Co-TiO_2 (b), 4%Co-TiO_2 (c), and 6%Co-TiO_2 (d).

4.6 Photocatalytic activity test

Photocatalytic activity of the synthesized TiO_2 and Co-doped TiO_2 samples was performed by the degradation of MB in aqueous solution under visible light irradiation. MB shows a maximum absorption at about 664 nm. Figure 17(a–d) shows the decomposition of MB in aqueous solution in the presence of TiO_2 and Co-doped TiO_2 photocatalyst. As we seen from the graph, intensity of single oxide (TiO_2) was high this indicates less degradation of MB. But when doping of different ratios (2%Co-TiO_2, 4%Co-TiO_2, and 6%Co-TiO_2) were used, the absorbance were decreased with irrespective increasing ratios of dopant, which implies high degradation of MB.

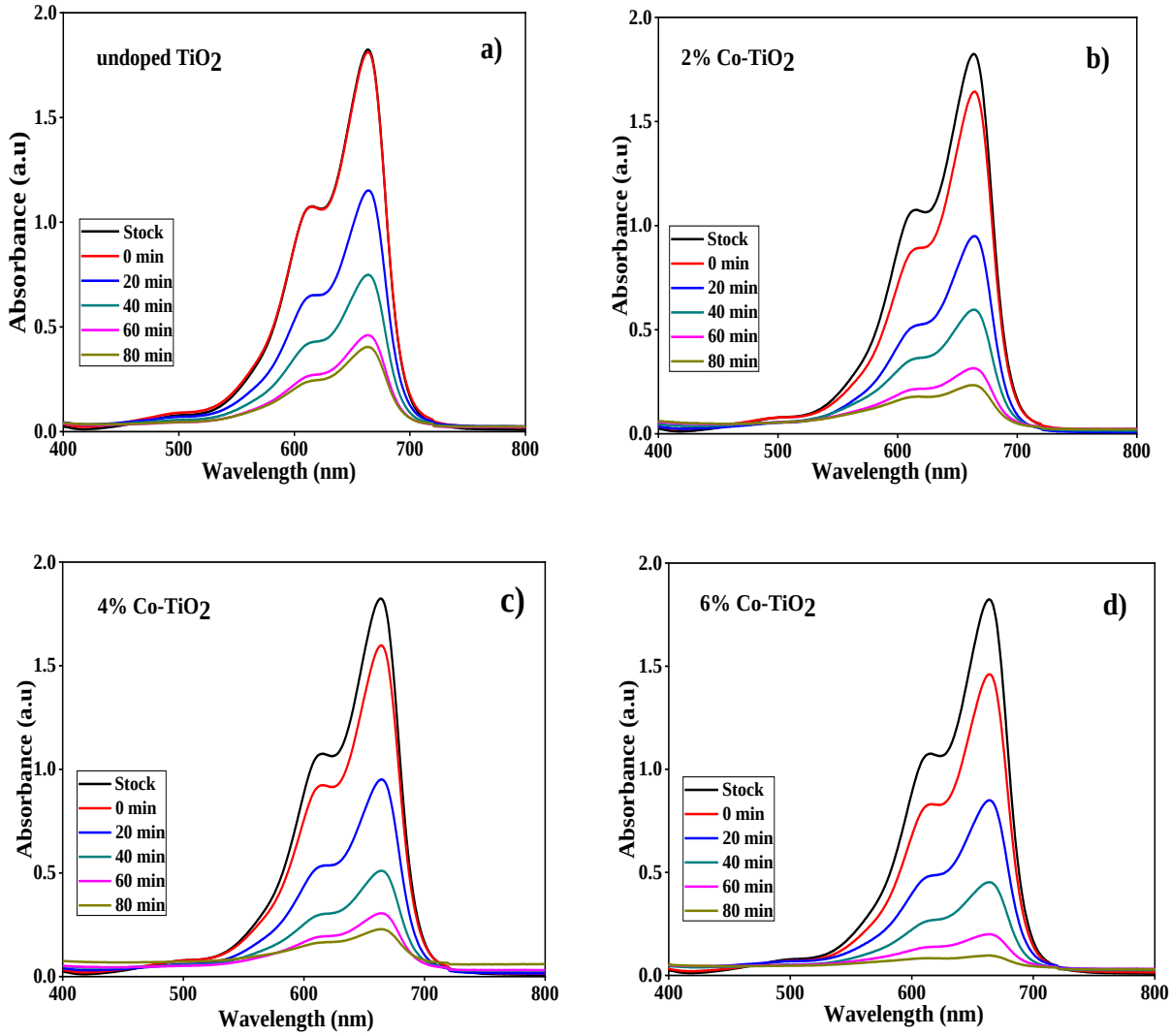

Figure 17: UV-Visible spectra showing the reduction in the intensity of MB dye solution under visible light irradiation by using catalyst TiO_2 (a), 2%Co-TiO_2 (b), 4%Co-TiO_2 (c), and 6%Co-TiO_2 (d).

The increase in photocatalytic activity exhibited by 2%Co-TiO_2, 4%Co-TiO_2, and 6%Co-TiO_2 appears to be associated with the narrowing of the band gap and an extension in the lifetime of photogenerated (e^- /h^+) pairs (El Mragui et al., 2021).

The determination of the pseudo-first-order rate constant for MB degradation in photocatalytic reaction was carried out by plotting $\ln(C/C_0)$ versus irradiation time (t) (equation 13). The plot of $\ln(C/C_0)$ Vs irradiation time as shown in Figure 18(a) gives the rate constant for the synthesized samples. The rate constant for undoped TiO_2, 2%Co-TiO_2, 4%Co-TiO_2, and 6%Co-TiO_2 NPs were

found to be 0.017, 0.022, 0.023, and 0.031 min^{-1} respectively. Among them, the 6%Co-TiO_2 possess the highest degradation rate constant. In addition to this, the pseudo-second-order rate constant was explored using the plot of 1/Ct Vs irradiation time for the degradation of MB (equation 14).

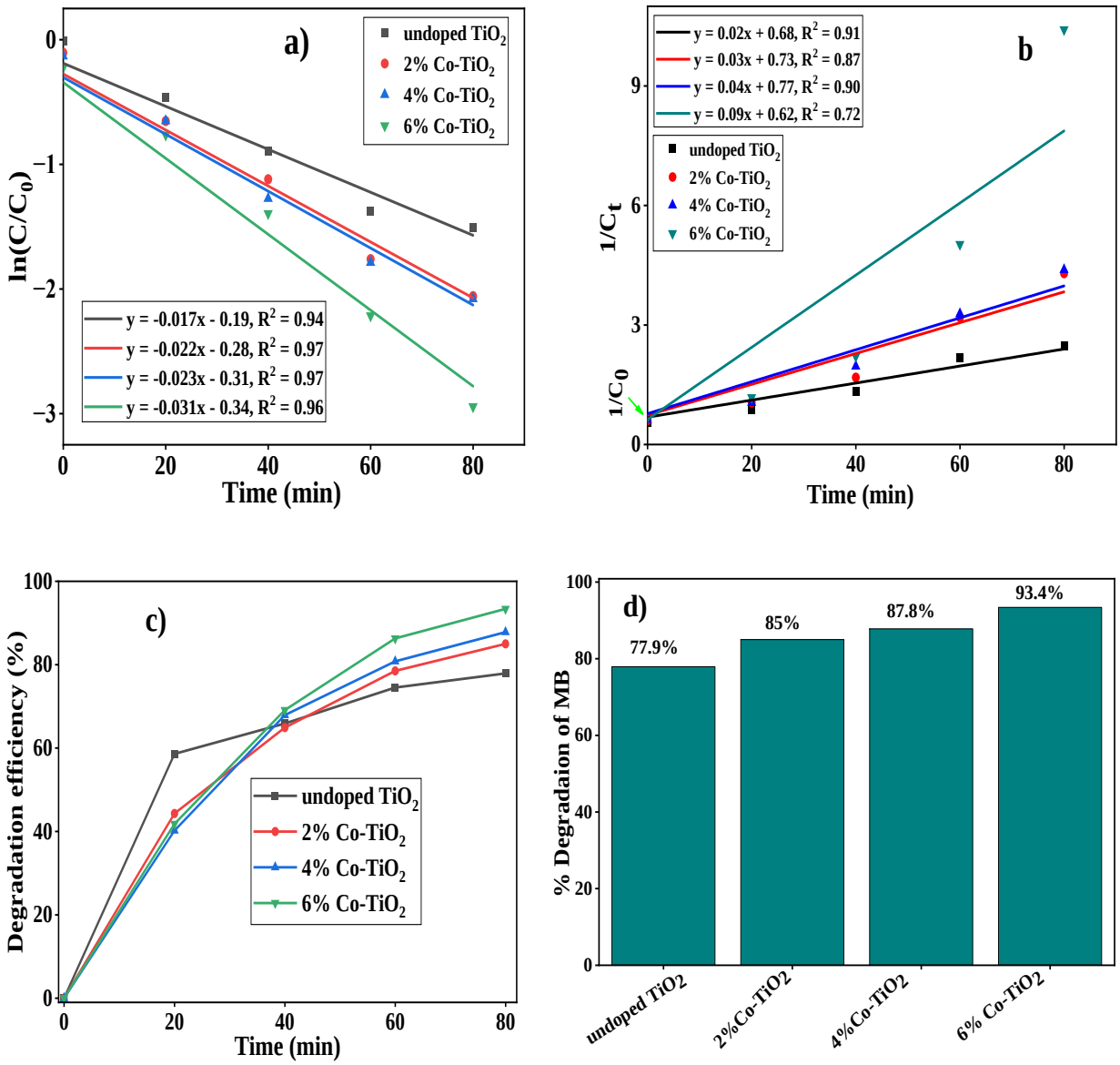

Figure 18: plot of ln(C/C0) Vs. times (a), plot of 1/Ct Vs. times (b), Plot of percentage of degradation Vs. times of MB with different samples (c), and corresponding degradation efficiency (d).

As it can be seen from Figure 18(a and b), the correlation constant (R^2) for the fitted lines are greater than 0.94 in pseudo first order model for the undoped TiO_2 and Co-doped TiO_2 NPs. While in pseudo second order model the correlation constant (R^2) for the fitted lines are less than 0.91. Therefore, the photodegradation of MB by the undoped TiO_2 and Co-doped TiO_2 NPs follows a pseudo-first-order kinetics model (L. T. Nguyen et al., 2019). Figure 18(c and d) shows percent photocatalytic degradation of MB. The 6%Co-TiO_2 had the highest MB degrading efficiency (93.4%) after 80 min of visible light exposure. Hence, the 6%Co-TiO_2 catalyst was used for further photocatalytic performance study.

4.6.1 Effect of initial dye concentration

The effect of different initial concentrations of MB was tested for the photocatalytic activity with 6%Co-TiO_2 catalyst under the visible light irradiation with time intervals of 0 to 80 min as shown in Figure 19(a-c). The effect of initial MB concentration was investigated by using 10 ppm, 15 ppm and 20 ppm of MB concentration with 20 mg of 6%Co-TiO_2 catalyst under neutral condition. The results showed that the degradation efficiency is high at low concentrations of organic dyes and gradually decreases as the dye concentration increases. This could be resulted from the increase in the thickness of dye layer adsorbed on the surface; hence the radiation may not interact with the catalyst. As the dye concentration increases, more hydroxyl radicals are required for the degradation of dye molecules and while, the formation of hydroxyl radicals on the catalyst surface decreased for a given light intensity, catalyst dose and irradiation time.

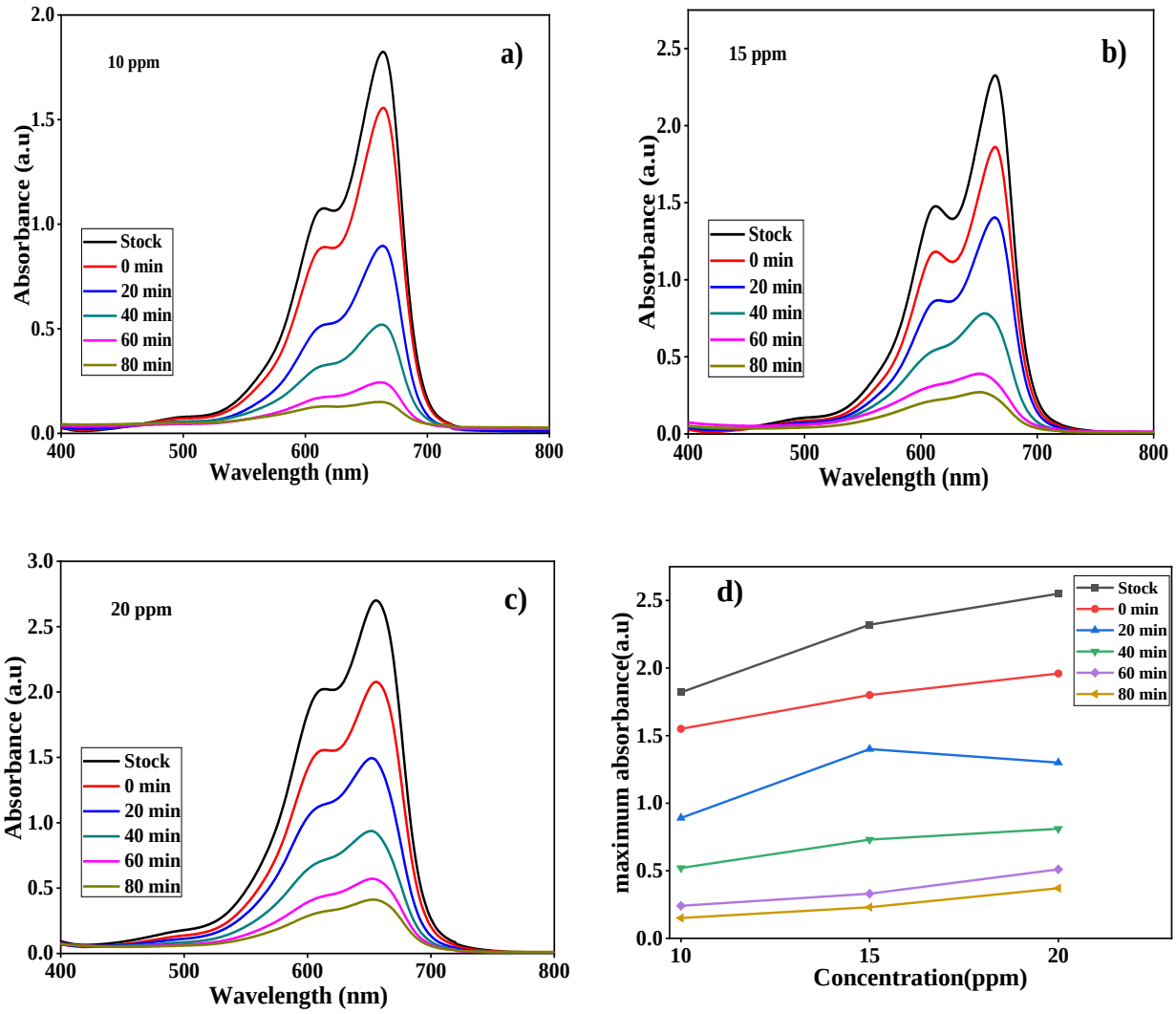

Figure 19: UV-Visible spectra of MB with different initial concentration of 10 ppm (a), 15 ppm (b), 20 ppm (c), with 20 mg of catalyst at pH 7 under visible light irradiation with reaction time interval 0 to 80 min, and Plot of maximum absorbance Vs. concentration (d)

Therefore the hydroxyl radicals produced are insufficient for the degradation of dye at high concentration. Hence, photodegradation efficiency reduces as the concentration of dye increases Figure 20(c and d) (Isai & Shrivastava, 2019). Figure 20(a and b) illustrated that, the reaction rates of both pseudo-first-order and pseudo second order kinetics model were found to decrease with increasing MB concentration and .the correlation constant (R^2) shows the reaction followed the pseudo-first-order kinetic model.

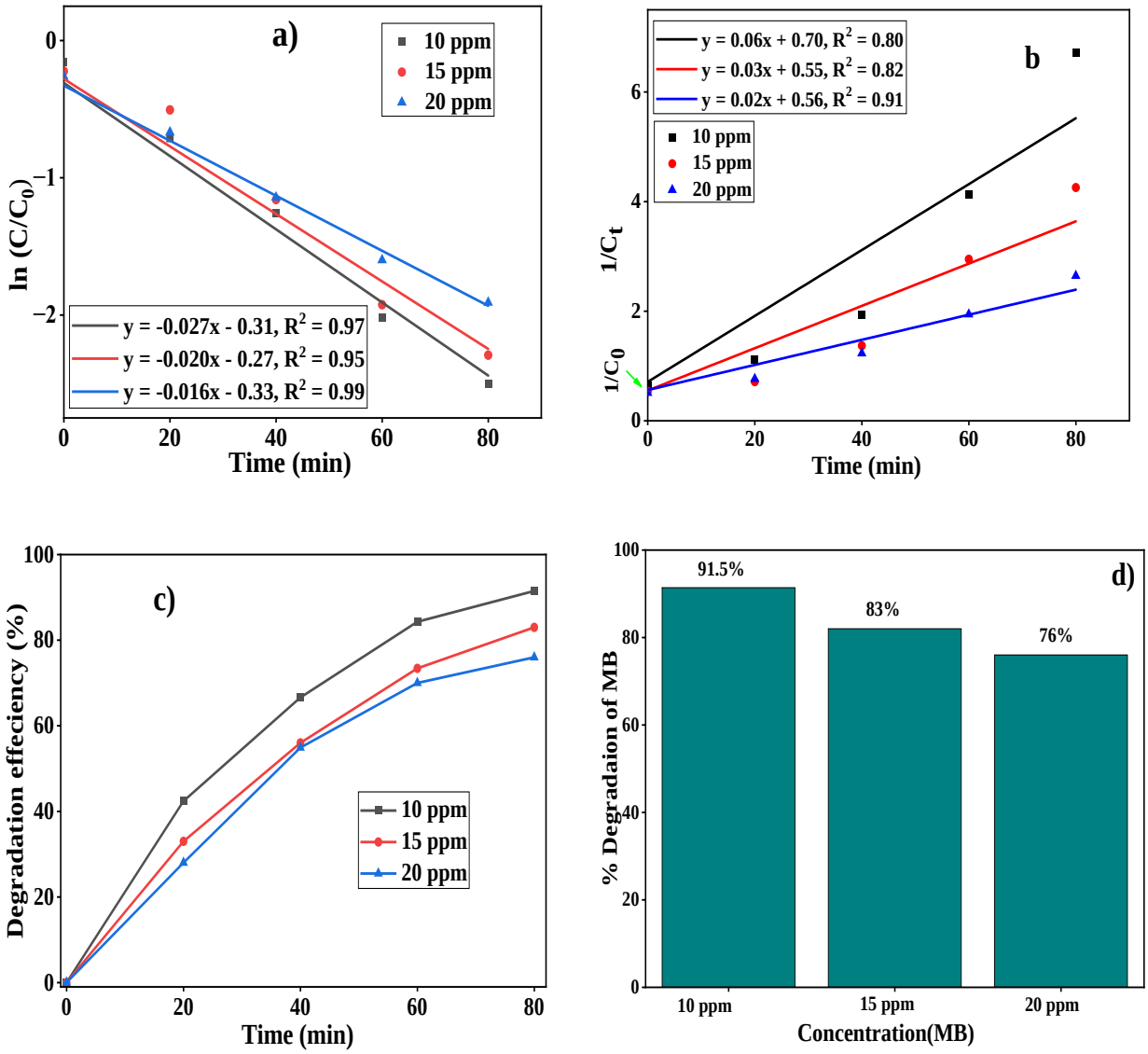

Figure 20: plot of ln(C/C_0) vs. times (a), plot of 1/Ct Vs. times (b), Plot of percentage of degradation vs. times of MB with different initial concentration of 10 ppm, 15 ppm, and 20 ppm (c), and corresponding degradation efficiency of catalyst (d).

4.6.2 Effect of pH

The effect of pH was studied for the photocatalytic degradation of MB solution with 6%Co-TiO_2 catalyst. In order to demonstrate the photocatalytic degradation of MB, different pH sample solutions of 5, 7, and 9 were used along with 20 mg of 6%Co-TiO_2 catalyst and 10 ppm of MB solution under visible light irradiation in a time intervals of 0 to 80 min as shown in Figure 21(a-c).

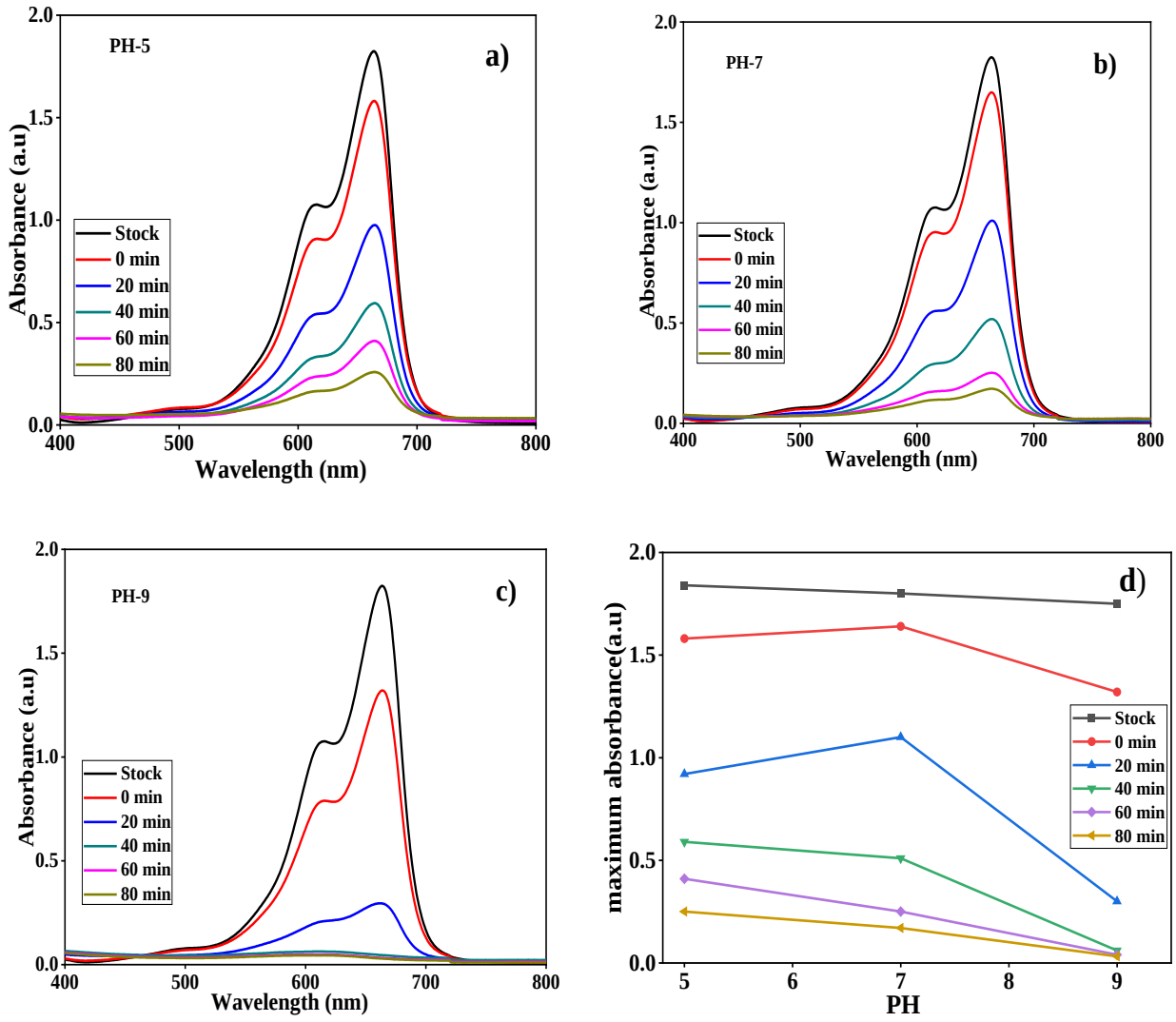

Figure 21: UV-Visible spectra of MB with different pH of 5 (a), 7 (b), 9 (c), with 20 mg of catalyst and 10 ppm of MB under visible light irradiation with reaction time interval 0 to 80 min, and Plot of maximum absorbance Vs. pH (d).

The degradation efficiency of the catalyst was increased as the sample solution become basic. The increase in percent degradation was from 83.6% to 96% as pH gets increased from 5 to 9 as depicted in figure 22(c and d). This is based on the variation in electrostatic forces between the catalyst surface and MB molecules at various pH levels. In an alkaline medium, the catalyst's surface is negatively charged while in an acidic medium, the surface of the catalyst become positively charged. MB is a cationic dye, so when it dissolves in water, its structure becomes positively charged. The surface interaction of the positively charged MB and the negatively

charged catalyst surface increases at higher pH. Therefore, the rate of MB degradation is higher in alkaline media due to an increase in opposite-charge interactions between the dye and catalyst surface (Prabakaran & Pillay, 2019). The rate constant "K" values for pH 5,7, and 9 as shown in Figure 22(a and b) for both pseudo-first-order and pseudo second order kinetics model displayed that, the higher degradation at higher pH value was confirmed by the higher rate constant for pH 9. The correlation constant (R^2) indicated in Figure 22(a and b) showed the degradation reaction followed the pseudo-first order kinetics model.

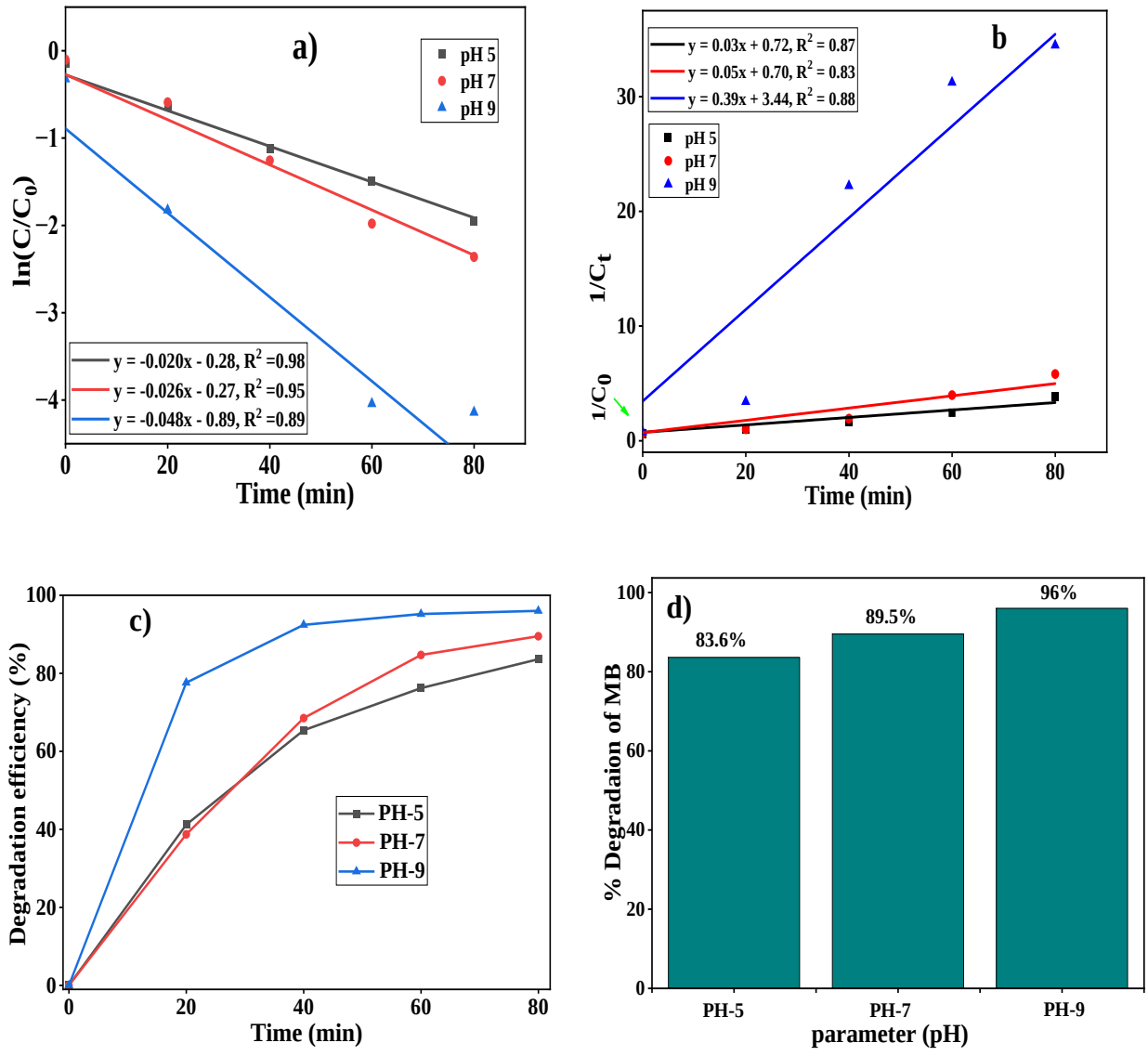

Figure 22: plot of $\ln(C/C_0)$ vs. times (a), plot of 1/Ct Vs. times (b), Plot of percentage of degradation vs. times of MB with different pH of 5, 7, and 9 (c), and corresponding degradation efficiency of catalyst (d).

4.6.3 Effect of catalyst dosage

Figure 23(a-d) shows the effect of dosage of 6%Co-TiO_2 catalyst on the photocatalytic degradation of MB under visible light irradiation in a time interval of 0 to 80 min. The influence of the catalyst dosage on the degradation of MB using 6%Co-TiO_2 catalyst was studied using 10 mg, 20 mg, 30 mg, and 50 mg of catalyst under neutral conditions with an initial MB concentration of 10 ppm.

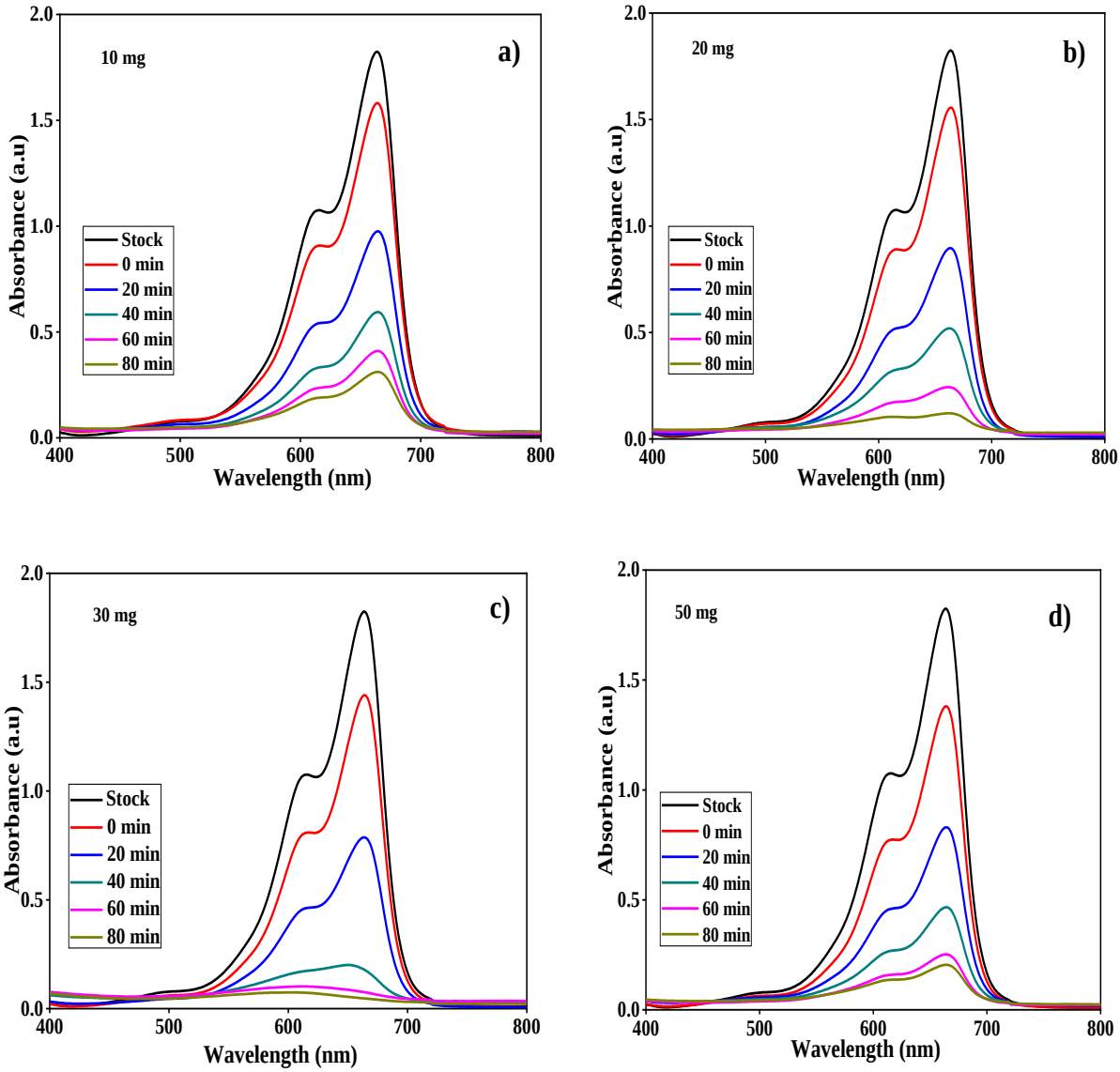

Figure 23: UV-Visible spectra of MB with different catalyst of 6%Co-TiO_2 10 mg (a), 20 mg (b), 30 mg (c), and 50 mg (d) with 10 ppm of MB at pH 7 under the visible light irradiation with reaction time interval 0 to 80 min.

The results showed that an increase in the degradation efficiency was observed with the increase in catalyst dosage up to 30 mg (Figure 24). This could be due to the presence of more active sites on the catalyst, which can adsorb more photons; and produces more OH• radicals and positive holes under irradiation. These hydroxyl radicals and positive holes involves in the photocatalytic reaction, and thus, the rate of dye degradation increased.

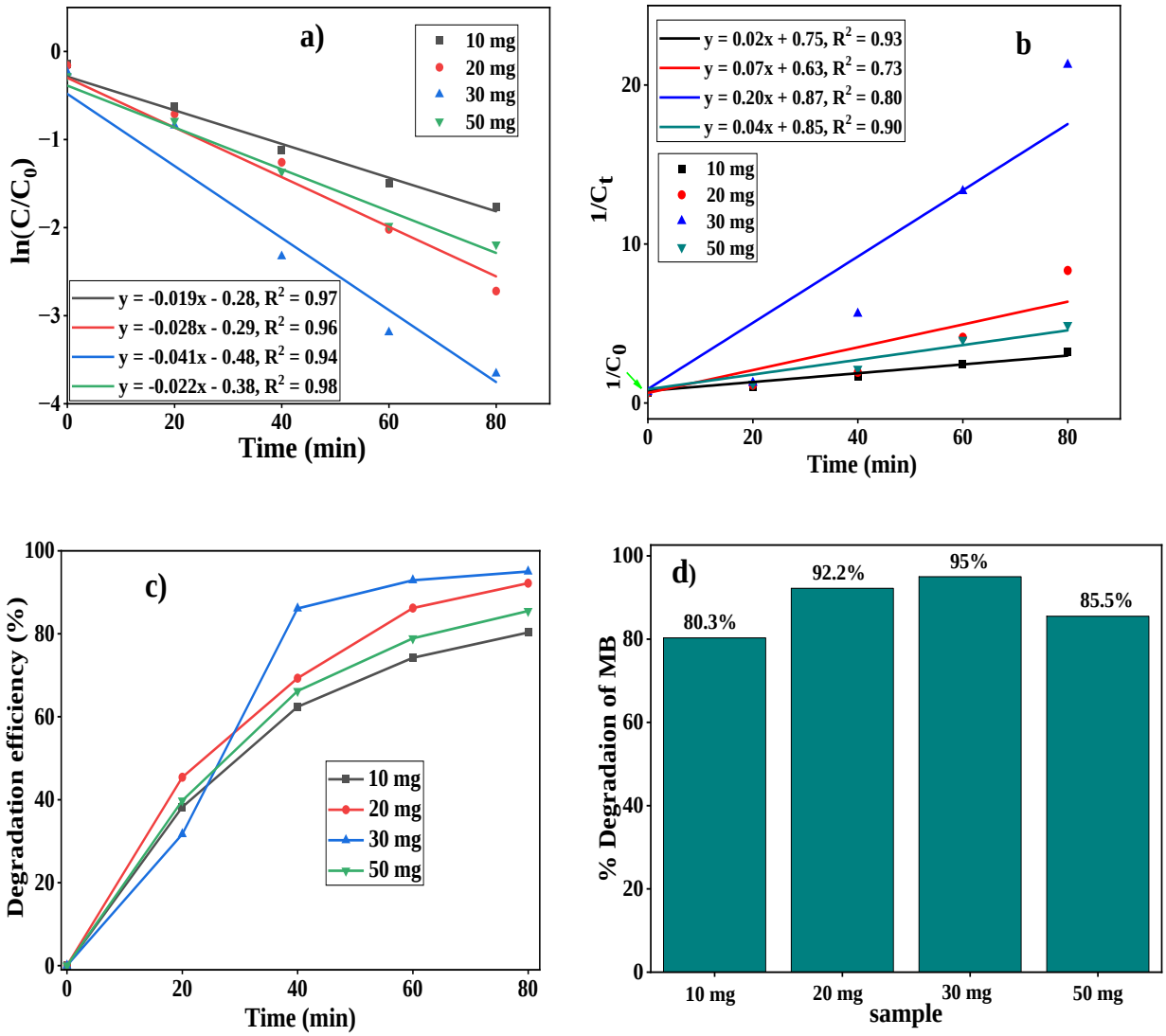

Figure 24: plot of ln(C/C_0) vs. times (a), plot of 1/Ct Vs. times (b), Plot of percentage of degradation vs. times of MB with different catalyst of 6%Co-TiO_2 10 mg, 20 mg, 30 mg, and 50 mg (c), and corresponding degradation efficiency of catalyst (d).

At higher catalyst dose (50 mg) the percent degradation of MB decreased because the active site of the catalyst collide and lose their activity. Moreover, it should be noticed that the reduction in

the percent degradation at higher catalyst loading may be also related to increased scattering and turbidity effects, which does not allow the penetration of light into all available surface of particles (Çağlar et al., 2020; Reza, Kurny, & Gulshan, 2017).

4.7 Antibacterial studies

The antibacterial activity of the synthesized TiO_2 and Co-doped TiO_2 NPs was investigated against the Gram-negative bacterial species (*Escherichia coli, Pseudomonas aeruginosa*) and Gram-positive bacterial species (*Staphylococcus aureus, and Streptococcus pyogenes*) compared to the standard drug ciprofloxacin through the disc diffusion method. The zone of inhibition values was measured as shown in Figure 25 and the results are given in Table 2.

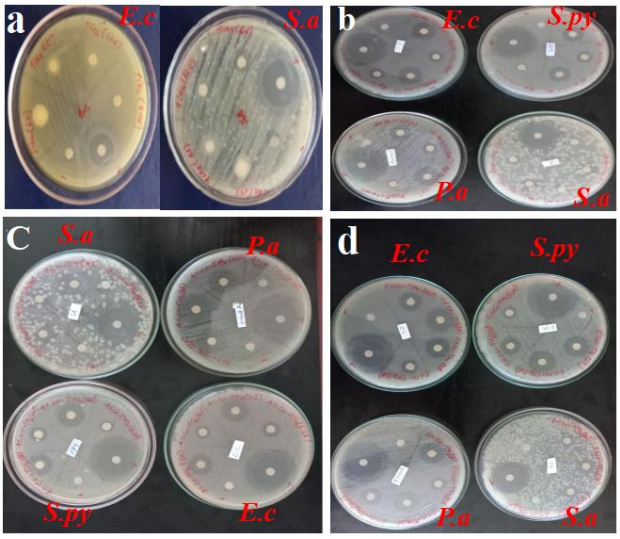

Figure 25: The antibacterial activity of the NPs TiO_2 (a), 2%Co-TiO_2 (b), 4%Co-TiO_2 (c), and 6%Co-TiO_2 (d) against G+ and G- bacterial strains.

The result showed that all the synthesized NPs have shown considerable antibacterial activity against all four pathogenic strains. The inhibition zone of bacterial strains increase as the concentration of dopant increases. Undoped TiO_2 showed the minimum zone of inhibition against *S. aureus* which is 6.5 mm. Relative to undoed TiO_2, 2% Co-TiO_2 and 4% Co-TiO_2 NPs exhibited improved antibacterial activity with the highest zone of inhibition recorded at 50 mg/mL against *E. coli* and *P. aeruginosa* which is 16 mm and 15 mm, and 18 mm and 15 mm respectively. However, the 6% Co-TiO_2 NPs has shown the highest zones of inhibition against all antibacterial

strains except *S. aureus*. The highest zone of inhibition by the 6% Co-TiO_2 NPs was recorded against Gram-negative bacteria *E. coli* which is 22 mm.

Table 2: Zone of inhibition (mm) of the synthesized NPs against bacterial strains.

Sample NMs	Conc. (mg/mL)	Bacteria Species and Zone of Inhibitions in mm			
		E. coli	*P. aeruginosa*	*S. aureus*	*S. pyogen*
undoped TiO_2	50	8	7	6.5	7
	25	7	6	6	6
	12.5	6	6	6	6
	6.25	6	6	6	6
	+ ve control	24	24	25	26
2% Co-TiO_2	50	16	15	11	12
	25	14	13	10	11
	12.5	12	11	8	9
	6.25	9	8	7	8
	+ ve control	26	25	22	26
4% Co-TiO_2	50	18	15	12	14
	25	16	14	12	13
	12.5	12	12	9	10
	6.25	10	9	7	8
	+ ve control	24	26	22	28
6% Co-TiO_2	50	22	20	14	18
	25	18	18	12	18
	12.5	16	15	11	14
	6.25	12	12	8	11
	+ve control)	25	28	26	26

The antibacterial activity of the 6% Co-TiO_2 NPs was compared with ciprofloxacin as the positive control and found to have comparable values. The increase in antibacterial activity with increase in the Co content can be attributed to superior lifetime of free charge carriers. Increasing the Co

content in TiO_2 increases the metal trap states thus lowering the recombination rate and thus increasing the antibacterial activity of Co-TiO_2 NPs with increase in the Co concentration (Ali et al., 2020).

While comparing the gram-positive and gram-negative bacteria, it has been observed that the inhibition zone is higher in gram- negative (*E. coli and P. aeruginosa*) bacteria than those of gram-positive bacteria (*S. aureus and S. pyogen*). The difference in antibacterial activity is due to their difference in membrane structure (Gram-positive and Gram-negative). The *S. aureus and S. pyogen* (Gram-positive) bacteria have a thick peptidoglycan layer, whereas, peptidoglycan layer in the *E. coli and P. aeruginosa* (Gram-negative) bacteria is thinner but surrounded by a lipid layer outside. According to several studies, green synthesized TiO_2 and Co-doped TiO_2 NPs shows antibacterial activity because biomolecules obtained from the plant extract are giving excess electron to TiO_2 and Co-doped TiO_2 NPs and result in the formation of superoxide radicals O_2^- , and the superoxide radicals produce reactive oxygen species (ROS) in bacterial cell. That ROS is used to break the bacterial cell membrane (Figure 26). As the superoxide radical production increased, ROS production also increased. These are all of the reasons for electron production from TiO_2 and Co-doped TiO_2 NPs, and as a result, TiO_2 and Co-doped TiO_2 NPs show antibacterial activity against both Gram-negative and Gram-positive bacteria strains (H. Zhang & Chen, 2009).

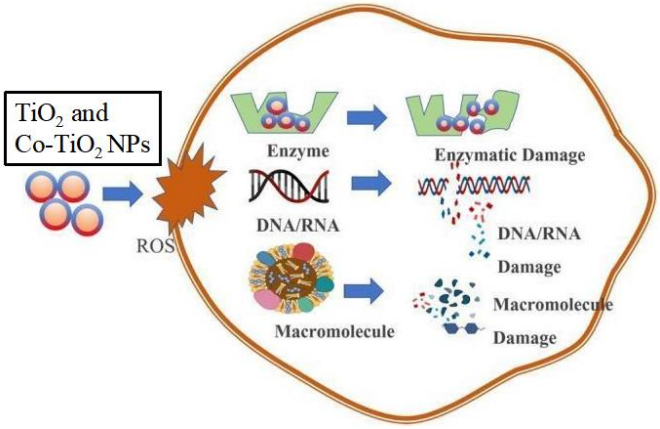

Figure 26: Schematic diagram showing the mechanism of antibacterial activity of TiO_2 and Co-doped TiO_2 NPs.

5. Conclusion and Recommendation

5.1 Conclusions

TiO_2 and Co-doped TiO_2 NPs were effectively synthesized by using *Millettia ferruginea* leaf extract as a green reducing, stabilizing and capping agent via co-precipitation technique. The synthesized NPs were characterized by TGA, XRD, UV-Vis DRS, FTIR, and SEM. Both undoped TiO_2 and Co-doped TiO_2 NPs were assessed for their photocatalytic activity. The result showed that the 6%Co-TiO_2 NPs exhibited higher photocatalytic degradation efficiency compared with the other synthesized NPs. The doped samples shows good photocatalytic activity toward the degradation of MB dye under visible light irradiation than undoped TiO_2 NPs. Among the doped NPs, 6% Co-TiO_2 NPs exhibited higher photocatalytic degradation efficiency (93.4%) after 80 min under visible light. Different parameters affecting the photocatalytic degradation of MB were also studied. It is found that pH of the dye solution, initial concentration of dye solution, and catalyst loading have a great influence on the photocatalytic performance. The optimum working conditions are at pH 9 of the dye solution, 10 ppm of dye concentration with 20 mg of catalyst that give 96% degradation of MB dye in 80 min under visible light. The antibacterial analysis showed that the 6% Co-TiO_2 NPs was the most effective compared to other synthesized NPs. Thus, on account of the remarkable photocatalytic activity and antibacterial performance of the 6% Co-TiO_2 NPs, it may be applied for the bacterial disinfection of wastewater and the photodegradation of numerous organic pollutants.

5.2 Recommendations

Future studies should consider the characterization of the synthesized NMs by energy-dispersive X-ray spectroscopy, transmission electron microscopy, and Brunauer-Emmett-Teller to determine their chemical composition, particle size, and surface properties. Moreover, it is important to investigate the practical application of the binary NPs for the removal of MB and other pollutants in real wastewater samples.

Research Fund Acknowledgment

This research project is funded by Adama Science and Technology University under the grant number ASTU/ SM-R/688/23, Adama, Ethiopia.

References

Abou El-Nour, K. M., Eftaiha, A. a., Al-Warthan, A., & Ammar, R. A. (2010). Synthesis and applications of silver nanoparticles. *Arabian journal of chemistry, 3*(3), 135-140.

Adyani, S. M., & Ghorbani, M. (2018). A comparative study of physicochemical and photocatalytic properties of visible light responsive Fe, Gd and P single and tri-doped TiO_2 nanomaterials. *Journal of Rare Earths, 36*(1), 72-85.

Ahmed, S., Ahmad, M., Swami, B. L., & Ikram, S. (2016). Green synthesis of silver nanoparticles using Azadirachta indica aqueous leaf extract. *Journal of radiation research and applied sciences, 9*(1), 1-7.

Ahmed, S. N., & Haider, W. (2018). Heterogeneous photocatalysis and its potential applications in water and wastewater treatment: a review. *Nanotechnology, 29*(34), 54-72.

Akbar, L., Ali, K., Sajjad, M., Sattar, A., Saleem, B., Amjad, U. Tahir, M. (2020). Enhancement in optical properties of cobalt doped TiO_2 nanoparticles. *Dig. J. Nanomater. Biostructures, 15*, 329-335.

Ali, M., Hussain, R., Tariq, F., Noreen, Z., Toufiq, A. M., Bokhari, H.Rahman, S. U. (2020). Highly effective visible light-activated cobalt-doped TiO_2 nanoparticles for antibacterial coatings against Campylobacter jejuni. *Applied Nanoscience, 10*, 1005-1012.

Alkaykh, S., Mbarek, A., & Ali-Shattle, E. E. (2020). Photocatalytic degradation of methylene blue dye in aqueous solution by $MnTiO_3$ nanoparticles under sunlight irradiation. *Heliyon, 6*(4), e03663.

Alothman, Z. A., Badjah, A. Y., Alharbi, O. M., & Ali, I. (2021). Cobalt doping of titanium oxide nanoparticles for atenolol photodegradation in water. *Environmental Science and Pollution Research, 28*(6), 7423-7430.

Ameta, R., Solanki, M. S., Benjamin, S., & Ameta, S. C. (2018). Photocatalysis. In *Advanced oxidation processes for waste water treatment* (pp. 135-175).

Anigol, L. B., Charantimath, J. S., & Gurubasavaraj, P. M. (2017). Effect of concentration and pH on the size of silver nanoparticles synthesized by green chemistry. *Org. Med. Chem. Int. J, 3*(5), 1-5.

Annu, A. A., & Ahmed, S. (2018). Green synthesis of metal, metal oxide nanoparticles, and their various applications. *Handbook of Ecomaterials, 2018*, 1-45.

Ansari, S. A., Khan, M. M., Ansari, M. O., & Cho, M. H. (2016). Nitrogen-doped titanium dioxide (N-doped TiO_2) for visible light photocatalysis. *New Journal of Chemistry*, *40*(4), 3000-3009.

Arda, L., Acikgoz, M., Aktas, Y., Cakiroglu, O., & Dogan, N. (2015). Structural and magnetic properties of Co-doped Er_2O_3 nanoparticles. *Journal of Magnetism and Magnetic Materials, 373*, 65-67.

Baek, Y.-W., & An, Y.-J. (2011). Microbial toxicity of metal oxide nanoparticles (CuO, NiO, ZnO, and Sb_2O_3) to Escherichia coli, Bacillus subtilis, and Streptococcus aureus. *Science of The Total Environment*, *409*(8), 1603-1608.

Bai, N., Liu, X., Li, Z., Ke, X., Zhang, K., & Wu, Q. (2021). High-efficiency TiO_2/ZnO nanocomposites photocatalysts by sol–gel and hydrothermal methods. *Journal of Sol-Gel Science and Technology*, *99*(1), 92-100.

Basavarajappa, P. S., Patil, S. B., Ganganagappa, N., Reddy, K. R., Raghu, A. V., & Reddy, C. V. (2020). Recent progress in metal-doped TiO_2, non-metal doped/codoped TiO2 and TiO_2 nanostructured hybrids for enhanced photocatalysis. *International journal of hydrogen energy*, *45*(13), 7764-7778.

Bayda, S., Adeel, M., Tuccinardi, T., Cordani, M., & Rizzolio, F. (2019). The history of nanoscience and nanotechnology: from chemical–physical applications to nanomedicine. *Molecules*, *25*(1), 112-120.

Bekele, E. T., Gonfa, B. A., Zelekew, O. A., Belay, H. H., & Sabir, F. K. (2020). Synthesis of titanium oxide nanoparticles using root extract of Kniphofia foliosa as a template, characterization, and its application on drug resistance bacteria. *Journal of Nanomaterials*, *2020*, 1-10.

Biru, M., Qaderi, J., Mamat, C., & Jalil, A. A. (2021). Preparation and characterization of copper, iron, and nickel doped titanium dioxide photocatalysts for decolorization of methylene blue. *Sains Malaysiana*, *50*(1), 135-149.

Botsa, S. M., Seetharam, P., Raju, I. M., Suresh, P., Satyanarayana, G., Sambasivam, S., . . . Tejeswararao, D. (2022). Nanohybrid material of Co–TiO_2 and optical performance on methylene blue dye under visible light illumination. *Hybrid Advances, 1*, 100008.

Budarz, J. F., Cooper, E. M., Gardner, C., Hodzic, E., Ferguson, P. L., Gunsch, C. K., & Wiesner, M. R. (2019). Chlorpyrifos degradation via photoreactive TiO_2 nanoparticles: assessing the

impact of a multi-component degradation scenario. *Journal of hazardous materials, 372*, 61-68.

Çağlar Yılmaz, H., Akgeyik, E., Bougarrani, S., El Azzouzi, M., & Erdemoğlu, S. (2020). Photocatalytic degradation of amoxicillin using Co-doped TiO_2 synthesized by reflux method and monitoring of degradation products by LC–MS/MS. *Journal of Dispersion Science and Technology, 41*(3), 414-425.

Cahino, A. M., Loureiro, R. G., Dantas, J., Madeira, V. S., & Fernandes, P. C. R. (2019). Characterization and evaluation of ZnO/CuO catalyst in the degradation of methylene blue using solar radiation. *Ceramics International, 45*(11), 13628-13636.

Cepoi, L., Rudi, L., Chiriac, T., Codreanu, S., & Valuţa, A. (2016). Biological methods of wastewater treatment. *Cyanobacteria for Bioremediation of Wastewaters*, 45-60.

Dakroury, G., Maree, R., El-Shazly, E., & Allan, K. (2022). Synthesize of poly (acrylamide-co-itaconic/TiO_2) nanocomposite for Ce (III) sorption from monazite leachate. *Journal of Polymers and the Environment*, 1-17.

Donga, C., Mishra, S. B., Abd-El-Aziz, A. S., & Mishra, A. K. (2021). Advances in graphene-based magnetic and graphene-based/TiO_2 nanoparticles in the removal of heavy metals and organic pollutants from industrial wastewater. *Journal of Inorganic and Organometallic Polymers and Materials, 31*(2), 463-480.

Dubey, M., Kumar, R., Srivastava, S. K., & Joshi, M. (2021). Visible light induced photodegradation of chlorinated organic pollutants using highly efficient magnetic Fe_3O_4/TiO_2 nanocomposite. *Optik, 243*, 167309.

Dunnill, C. W., Kafizas, A., & Parkin, I. P. (2012). CVD production of doped titanium dioxide thin films. *Chemical Vapor Deposition, 18*(4-6), 89-101.

El Mragui, A., Zegaoui, O., Daou, I., & Esteves da Silva, J. C. G. (2021). Preparation, characterization, and photocatalytic activity under UV and visible light of Co, Mn, and Ni mono-doped and (P, Mo) and (P, W) co-doped TiO_2 nanoparticles: A comparative study. *Environmental Science and Pollution Research, 28*, 25130-25145.

Faucon, M.-P., Pourret, O., & Lange, B. (2021). Element Case Studies: Cobalt. In *Agromining: Farming for Metals* (pp. 385-391).

Feiona, T. A., Sabeena, G., Bagavathy, M. S., Pushpalaksmi, E., Jenson Samraj, J., & Annadurai, G. (2021). Recent Advances in the Synthesis and Characterization of Nanoparticles: A

Green Adeptness for Photocatalytic and Antibacterial Activity. *Nature Environment & Pollution Technology, 20*(2) 6-19.

Fulekar, J., Dutta, D. P., Pathak, B., & Fulekar, M. H. (2018). Novel microbial and root mediated green synthesis of TiO_2 nanoparticles and its application in wastewater remediation. *Journal of Chemical Technology & Biotechnology, 93*(3), 736-743.

Ghicov, A., Schmidt, B., Kunze, J., & Schmuki, P. (2007). Photoresponse in the visible range from Cr doped TiO_2 nanotubes. *Chemical Physics Letters, 433*(4-6), 323-326.

Goutam, S. P., Saxena, G., Roy, D., Yadav, A. K., & Bharagava, R. N. (2020). Green synthesis of nanoparticles and their applications in water and wastewater treatment. In *Bioremediation of industrial waste for environmental safety* (pp. 349-379).

Goutam, S. P., Saxena, G., Singh, V., Yadav, A. K., Bharagava, R. N., & Thapa, K. B. (2018). Green synthesis of TiO_2 nanoparticles using leaf extract of Jatropha curcas L. for photocatalytic degradation of tannery wastewater. *Chemical Engineering Journal, 336*, 386-396.

Guesh, K., Mayoral, A., Marquez-Alvarez, C., Chebude, Y., & Diaz, I. (2016). Enhanced photocatalytic activity of TiO_2 supported on zeolites tested in real wastewaters from the textile industry of Ethiopia. *Microporous and Mesoporous Materials, 225*, 88-97.

Guo, M., Song, W., Wang, T., Li, Y., Wang, X., & Du, X. (2015). Phenyl-functionalization of titanium dioxide-nanosheets coating fabricated on a titanium wire for selective solid-phase microextraction of polycyclic aromatic hydrocarbons from environment water samples. *Talanta, 144*, 998-1006.

He, J., Kumar, A., Khan, M., & Lo, I. M. (2021). Critical review of photocatalytic disinfection of bacteria: from noble metals-and carbon nanomaterials-TiO2 composites to challenges of water characteristics and strategic solutions. *Science of The Total Environment, 758*, 143-153.

Holkar, C. R., Jadhav, A. J., Pinjari, D. V., Mahamuni, N. M., & Pandit, A. B. (2016). A critical review on textile wastewater treatments: possible approaches. *Journal of environmental management, 182*, 351-366.

Humphries, R. M., Ambler, J., Mitchell, S. L., Castanheira, M., Dingle, T., Hindler, J. A., . . . Sei, K. (2018). CLSI methods development and standardization working group best practices

for evaluation of antimicrobial susceptibility tests. *Journal of clinical microbiology*, *56*(4), e01934-01917.

Ijadpanah-Saravi, H., Dehestaniathar, S., Khodadadi-Darban, A., Zolfaghari, M., & Saeedzadeh, S. (2016). Photocatalytic decomposition of cyanide in pure water by biphasic titanium dioxide nanoparticles. *Desalination and Water Treatment*, *57*(43), 20503-20510.

Iravani, S. (2011). Green synthesis of metal nanoparticles using plants. *Green Chemistry*, *13*(10), 2638-2650.

Iravani, S., Korbekandi, H., Mirmohammadi, S. V., & Zolfaghari, B. (2014). Synthesis of silver nanoparticles: chemical, physical and biological methods. *Research in pharmaceutical sciences*, *9*(6), 385-397.

Iravani, S., & Varma, R. S. (2020). Sustainable synthesis of cobalt and cobalt oxide nanoparticles and their catalytic and biomedical applications. *Green Chemistry*, *22*(9), 2643-2661.

Irshad, S., Siddiqui, B., ur. Rehman, A., Farooq, R. K., & Ahmed, N. (2022). Recent trends and development in targeted delivery of therapeutics through enzyme responsive intelligent nanoplatform. *International Journal of Polymeric Materials and Polymeric Biomaterials*, *71*(6), 403-413.

Isai, K. A., & Shrivastava, V. S. (2019). Photocatalytic degradation of methylene blue using ZnO and 2% Fe–ZnO semiconductor nanomaterials synthesized by sol–gel method: a comparative study. *SN Applied Sciences*, *1*, 1-11.

Ismail, H. H., Hasoon, S. A., & Saheb, E. J. (2019). The anti-Leishmaniasis activity of green synthesis silver oxide nanoparticles. *Annals of Tropical Medicine and Health*, *22*, 28-38.

Jadoun, S., Arif, R., Jangid, N. K., & Meena, R. K. (2021). Green synthesis of nanoparticles using plant extracts: A review. *Environmental Chemistry Letters*, *19*, 355-374.

Jalab, J., Abdelwahed, W., Kitaz, A., & Al-Kayali, R. (2021). Green synthesis of silver nanoparticles using aqueous extract of Acacia cyanophylla and its antibacterial activity. *Heliyon*, *7*(9), 8-33.

Jassal, P. S., Kaur, D., Prasad, R., & Singh, J. (2022). Green synthesis of titanium dioxide nanoparticles: Development and applications. *Journal of Agriculture and Food Research*, 100361.

Javed, A., QAMMAR, M., Khurram, R., Nisa, Z., & Nasir, H. (2021). Visible Light Active Nitrogen and Cobalt Co-doped TiO2 Nanoparticles: Synthesis, Characterization and Photocatalytic Activity. Research square, 9, 2-7.

Jayaseelan, C., Rahuman, A. A., Roopan, S. M., Kirthi, A. V., Venkatesan, J., Kim, S.-K.Siva, C. (2013). Biological approach to synthesize TiO_2 nanoparticles using Aeromonas hydrophila and its antibacterial activity. *Spectrochimica Acta Part A: Molecular and Biomolecular Spectroscopy, 107*, 82-89.

Jeyaraj, M., Gurunathan, S., Qasim, M., Kang, M.-H., & Kim, J.-H. (2019). A comprehensive review on the synthesis, characterization, and biomedical application of platinum nanoparticles. *Nanomaterials, 9*(12), 1719.

Karthikeyan, K., Nithya, A., & Jothivenkatachalam, K. (2017). Photocatalytic and antimicrobial activities of chitosan-TiO_2 nanocomposite. *International journal of biological macromolecules, 104*, 1762-1773.

Kashale, A. A., Rasal, A. S., Kamble, G. P., Ingole, V. H., Dwivedi, P. K., Rajoba, S. J.Ghule, A. V. (2019). Biosynthesized Co-doped TiO_2 nanoparticles based anode for lithium-ion battery application and investigating the influence of dopant concentrations on its performance. *Composites Part B: Engineering, 167*, 44-50.

Khan, I., Saeed, K., & Khan, I. (2019). Nanoparticles: Properties, applications and toxicities. *Arabian journal of chemistry, 12*(7), 908-931.

Khan, N. T., & Khan, M. J. (2020). Metallic nanoparticles fabrication methods–A brief overview. *SunKrist Nanotechnol. Nanosci. J, 2*, 1-6.

Khurana, C., Pandey, O., & Chudasama, B. (2015). Synthesis of visible light-responsive cobalt-doped TiO_2 nanoparticles with tunable optical band gap. *Journal of Sol-Gel Science and Technology, 75*, 424-435.

Koli, V. B., Ke, S.-C., Dodamani, A. G., Deshmukh, S. P., & Kim, J.-S. (2020). Boron-doped TiO_2-CNT nanocomposites with improved photocatalytic efficiency toward photodegradation of Toluene gas and photo-inactivation of Escherichia coli. *Catalysts, 10*(6), 632-641.

Kumar, H., Venkatesh, N., Bhowmik, H., & Kuila, A. (2018). Metallic nanoparticle: a review. *Biomedical Journal of Scientific & Technical Research, 4*(2), 3765-3775.

Kumar Teli, M., Mutalik, S., & Rajanikant, G. (2010). Nanotechnology and nanomedicine: going small means aiming big. *Current pharmaceutical design, 16*(16), 1882-1892.

Lakshmi, K. D., Rao, T. S., Padmaja, J. S., Raju, I. M., Alim, S. A., & Kalyani, P. (2018). Visible light driven mesoporous Mn and S co-doped TiO_2 nano material: Characterization and applications in photocatalytic degradation of indigocarmine dye and antibacterial activity. *Environmental nanotechnology, monitoring & management, 10*, 494-504.

Lim, J., & Hoffmann, M. R. (2020). Peroxymonosulfate (PMS) activation on cobalt-doped TiO_2 nanotubes: degradation of organics under dark and solar light irradiation conditions. *Environmental Science: Nano, 7*(5), 1602-1611.

Liou, J.-W., & Chang, H.-H. (2012). Bactericidal effects and mechanisms of visible light-responsive titanium dioxide photocatalysts on pathogenic bacteria. *Archivum immunologiae et therapiae experimentalis, 60*(4), 267-275.

Liu, Q., Zhou, Y., Lu, J., & Zhou, Y. (2020). Novel cyclodextrin-based adsorbents for removing pollutants from wastewater: a critical review. *Chemosphere, 241*, 125043.

Mais, L., Vacca, A., Mascia, M., Usai, E. M., Tronci, S., & Palmas, S. (2020). Experimental study on the optimisation of azo-dyes removal by photo-electrochemical oxidation with TiO_2 nanotubes. *Chemosphere, 248*, 125938.

Mansour, S. A., Farha, A., & Kotkata, M. (2019). Sol–Gel Synthesized Co-Doped Anatase TiO_2 Nanoparticles: Structural, Optical, and Magnetic Characterization. *Journal of Inorganic and Organometallic Polymers and Materials, 29*, 1375-1382.

Matheyarasu, R., Seshadri, B., Bolan, N. S., & Naidu, R. (2014). Impacts of abattoir waste-water irrigation on soil fertility and productivity.

Mittal, A. K., Chisti, Y., & Banerjee, U. C. (2013). Synthesis of metallic nanoparticles using plant extracts. *Biotechnology advances, 31*(2), 346-356.

Mugundan, S., Rajamannan, B., Viruthagiri, G., Shanmugam, N., Gobi, R., & Praveen, P. (2015). Synthesis and characterization of undoped and cobalt-doped TiO_2 nanoparticles via sol–gel technique. *Applied Nanoscience, 5*, 449-456.

Nadeem, M., Tungmunnithum, D., Hano, C., Abbasi, B. H., Hashmi, S. S., Ahmad, W., & Zahir, A. (2018). The current trends in the green syntheses of titanium oxide nanoparticles and their applications. *Green Chemistry Letters and Reviews, 11*(4), 492-502.

Nakamura, S., Sato, M., Sato, Y., Ando, N., Takayama, T., Fujita, M., & Ishihara, M. (2019). Synthesis and application of silver nanoparticles (Ag NPs) for the prevention of infection in healthcare workers. *International journal of molecular sciences, 20*(15), 3620.

Nankya, R., & Kim, K.-N. (2016). Sol–gel synthesis and characterization of Cu–TiO_2 nanoparticles with enhanced optical and photocatalytic properties. *Journal of Nanoscience and Nanotechnology, 16*(11), 11631-11634.

Nassar, M. Y., Ahmed, I. S., Mohamed, T. Y., & Khatab, M. (2016). A controlled, template-free, and hydrothermal synthesis route to sphere-like α-Fe_2O_3 nanostructures for textile dye removal. *Rsc Advances, 6*(24), 20001-20013.

Nguyen, L. T., Nguyen, L. T., Manh, N. C., Quoc, D. N., Quang, H. N., Nguyen, H. T.Bach, L. G. (2019). A facile synthesis, characterization, and photocatalytic activity of magnesium ferrite nanoparticles via the solution combustion method. *Journal of Chemistry, 2019*, 1-8.

Nguyen, T. M. H., & Bark, C. W. (2020). Synthesis of cobalt-doped TiO_2 based on metal–organic frameworks as an effective electron transport material in perovskite solar cells. *ACS omega, 5*(5), 2280-2286.

Osonga, F. J., Akgul, A., Yazgan, I., Akgul, A., Eshun, G. B., Sakhaee, L., & Sadik, O. A. (2020). Size and shape-dependent antimicrobial activities of silver and gold nanoparticles: A model study as potential fungicides. *Molecules, 25*(11), 2682.

Panhwar, S., Buledi, J. A., Mal, D., Solangi, A. R., Balouch, A., & Hyder, A. (2021). Importance and analytical perspective of green synthetic strategies of copper, zinc, and titanium oxide nanoparticles and their applications in pathogens and environmental remediation. *Current Analytical Chemistry, 17*(8), 1169-1181.

Patil, S. B., Basavarajappa, P. S., Ganganagappa, N., Jyothi, M., Raghu, A., & Reddy, K. R. (2019). Recent advances in non-metals-doped TiO2 nanostructured photocatalysts for visible-light driven hydrogen production, CO2 reduction and air purification. *International journal of hydrogen energy, 44*(26), 13022-13039.

Patra, J. K., & Baek, K.-H. (2014). Green nanobiotechnology: factors affecting synthesis and characterization techniques. *Journal of Nanomaterials, 20, 4-9*.

Piaskowski, K., Świderska-Dąbrowska, R., & Zarzycki, P. K. (2018). Dye removal from water and wastewater using various physical, chemical, and biological processes. *Journal of AOAC International, 101*(5), 1371-1384.

Prabakaran, E., & Pillay, K. (2019). Synthesis of N-doped ZnO nanoparticles with cabbage morphology as a catalyst for the efficient photocatalytic degradation of methylene blue under UV and visible light. *Rsc Advances, 9*(13), 7509-7535.

Pype, M.-L., Lawrence, M. G., Keller, J., & Gernjak, W. (2016). Reverse osmosis integrity monitoring in water reuse: The challenge to verify virus removal–A review. *Water research, 98*, 384-395.

Rani, M., & Shanker, U. (2020). Green synthesis of TiO_2 and its photocatalytic activity. In *Handbook of Smart Photocatalytic Materials* (pp. 11-61).

Raveau, B., & Seikh, M. M. (2015). Charge ordering in cobalt oxides: Impact on structure, magnetic and transport properties. *Zeitschrift für anorganische und allgemeine Chemie, 641*(8-9), 1385-1394.

Reza, K. M., Kurny, A., & Gulshan, F. (2017). Parameters affecting the photocatalytic degradation of dyes using TiO_2: a review. *Applied Water Science, 7*, 1569-1578.

Rojas-Andrade, M. D., Chata, G., Rouholiman, D., Liu, J., Saltikov, C., & Chen, S. (2017). Antibacterial mechanisms of graphene-based composite nanomaterials. *Nanoscale, 9*(3), 994-1006.

Sadanandam, G., Lalitha, K., Kumari, V. D., Shankar, M. V., & Subrahmanyam, M. (2013). Cobalt doped TiO_2: A stable and efficient photocatalyst for continuous hydrogen production from glycerol: Water mixtures under solar light irradiation. *International journal of hydrogen energy, 38*(23), 9655-9664.

Safoniuk, M. (2004). Wastewater engineering: Treatment and reuse. *Chemical engineering, 111*(7), 10-12.

Sahoo, M., Vishwakarma, S., Panigrahi, C., & Kumar, J. (2021). Nanotechnology: Current applications and future scope in food. *Food Frontiers, 2*(1), 3-22.

Sakhare, Y., Bhoraskar, S., Mathe, V., & Ubale, A. (2014). Electric field assisted enhanced photo catalytic activities of immobilized nano TiO_2 on porous silicon. *Materials Research Bulletin, 59*, 205-213.

Santhoshkumar, T., Rahuman, A. A., Jayaseelan, C., Rajakumar, G., Marimuthu, S., Kirthi, A. V. Kim, S.-K. (2014). Green synthesis of titanium dioxide nanoparticles using Psidium guajava extract and its antibacterial and antioxidant properties. *Asian Pacific journal of tropical medicine, 7*(12), 968-976.

Sathiyan, K., Bar-Ziv, R., Mendelson, O., & Zidki, T. (2020). Controllable synthesis of TiO_2 nanoparticles and their photocatalytic activity in dye degradation. *Materials Research Bulletin, 126*, 110842.

Saxena, G., & Bharagava, R. N. (2017). Organic and inorganic pollutants in industrial wastes: ecotoxicological effects, health hazards, and bioremediation approaches. In *Environmental pollutants and their bioremediation approaches* (pp. 23-56).

Seabra, A. B., & Durán, N. (2015). Nanotoxicology of metal oxide nanoparticles. *Metals, 5*(2), 934-975.

Selihin, N. M., & Tay, M. G. (2022). A review on future wastewater treatment technologies: micro-nanobubbles, hybrid electro-Fenton processes, photocatalytic fuel cells, and microbial fuel cells. *Water Science and Technology, 85*(1), 319-341.

Shafiq, I., Shafique, S., Akhter, P., Abbas, G., Qurashi, A., & Hussain, M. (2022). Efficient catalyst development for deep aerobic photocatalytic oxidative desulfurization: recent advances, confines, and outlooks. *Catalysis reviews, 64*(4), 789-834.

Shah, M., Fawcett, D., Sharma, S., Tripathy, S. K., & Poinern, G. E. J. (2015). Green synthesis of metallic nanoparticles via biological entities. *Materials, 8*(11), 7278-7308.

Shanaj, B., & John, X. (2016). Effect of calcination time on structural, optical and antimicrobial properties of nickel oxide nanoparticles. *J. Theor. Comput. Sci, 3*(2), 149-159.

Shenoy, R. U. K., Rama, A., Govindan, I., & Naha, A. (2022). The purview of doped nanoparticles: Insights into their biomedical applications. *OpenNano*, 100070.

Sicardi, S. (2020). Treatment of wastewater from textile dyeing by ozonization.

Simões, M. F., Ottoni, C. A., & Antunes, A. (2020). Biogenic metal nanoparticles: A new approach to detect life on Mars? *Life, 10*(3), 28.

Soman, B., Challagulla, S., Payra, S., Dinda, S., & Roy, S. (2018). Surface morphology and active sites of TiO_2 for photoassisted catalysis. *Research on Chemical Intermediates, 44*(4), 2261-2273.

Subramanian, A., Pan, Z., Li, H., Zhou, L., Li, W., Qiu, Y., . . . Zhang, Y. (2017). Synergistic promotion of photoelectrochemical water splitting efficiency of TiO_2 nanorods using metal-semiconducting nanoparticles. *Applied Surface Science, 420*, 631-637.

Sundrarajan, M., Bama, K., Bhavani, M., Jegatheeswaran, S., Ambika, S., Sangili, A. Sumathi, R. (2017). Obtaining titanium dioxide nanoparticles with spherical shape and antimicrobial

properties using M. citrifolia leaves extract by hydrothermal method. *Journal of Photochemistry and Photobiology B: Biology, 171*, 117-124.

Taoda, H. (2008). Development of TiO_2 photocatalysts suitable for practical use and their applications in environmental cleanup. *Research on Chemical Intermediates, 34*, 417-426.

Tarafdar, A., Raliya, R., Wang, W.-N., Biswas, P., & Tarafdar, J. (2013). Green synthesis of TiO_2 nanoparticle using Aspergillus tubingensis. *Advanced Science, Engineering and Medicine, 5*(9), 943-949.

Tauc, J., Grigorovici, R., & Vancu, A. (1966). Optical properties and electronic structure of amorphous germanium. *physica status solidi (b), 15*(2), 627-637.

Uddin, S., Safdar, L. B., Iqbal, J., Yaseen, T., Laila, S., Anwar, S. Quraishi, U. M. (2021). Green synthesis of nickel oxide nanoparticles using leaf extract of Berberis balochistanica: Characterization, and diverse biological applications. *Microscopy Research and Technique, 84*(9), 2004-2016.

Venturini, J., Bonatto, F., Guaglianoni, W. C., Lemes, T., Arcaro, S., Alves, A. K., & Bergmann, C. P. (2019). Cobalt-doped titanium oxide nanotubes grown via one-step anodization for water splitting applications. *Applied Surface Science, 464*, 351-359.

Verma, V., Al-Dossari, M., Singh, J., Rawat, M., Kordy, M. G., & Shaban, M. (2022). A Review on Green Synthesis of TiO_2 NPs: Photocatalysis and Antimicrobial Applications. *Polymers, 14*(7), 1444.

Vinatier, C., Mrugala, D., Jorgensen, C., Guicheux, J., & Noël, D. (2009). Cartilage engineering: a crucial combination of cells, biomaterials and biofactors. *Trends in biotechnology, 27*(5), 307-314.

Wang, J., Yao, J., Wang, L., Xue, Q., Hu, Z., & Pan, B. (2020). Multivariate optimization of the pulse electrochemical oxidation for treating recalcitrant dye wastewater. *Separation and Purification Technology, 230*, 115851.

Wang, L., Fu, X., Han, Y., Chang, E., Wu, H., Wang, H. Qi, X. (2013). Preparation, characterization, and photocatalytic activity of TiO_2/ZnO nanocomposites. *Journal of Nanomaterials, 13* 5-12.

Waris, A., Din, M., Ali, A., Afridi, S., Baset, A., Khan, A. U., & Ali, M. (2021). Green fabrication of Co and Co_3O_4 nanoparticles and their biomedical applications: A review. *Open life sciences, 16*(1), 14-30.

Wawrzkiewicz, M., Polska-Adach, E., & Hubicki, Z. (2019). Application of titania based adsorbent for removal of acid, reactive and direct dyes from textile effluents. *Adsorption, 25*(3), 621-630.

Wong, J. K. H., Tan, H. K., Lau, S. Y., Yap, P.-S., & Danquah, M. K. (2019). Potential and challenges of enzyme incorporated nanotechnology in dye wastewater treatment: A review. *Journal of environmental chemical engineering, 7*(4), 103261.

Xu, J., Shen, X., Wang, D., Zhao, C., Liu, Z., Pozdnyakov, I. P. Xia, J. (2018). Kinetics and mechanisms of pH-dependent direct photolysis of p-arsanilic acid under UV-C light. *Chemical Engineering Journal, 336*, 334-341.

Yadav, S., Tyagi, D., & Yadav, O. (2011). Equilibrium and kinetic studies on adsorption of aniline blue from aqueous solution onto rice husk carbon. *International Journal of Chemistry Research*, 59-64.

Yang, C., Xu, W., Nan, Y., Wang, Y., Hu, Y., Gao, C., & Chen, X. (2020). Fabrication and characterization of a high performance polyimide ultrafiltration membrane for dye removal. *Journal of colloid and interface science, 562*, 589-597.

Yogalakshmi, K. N., Das, A., Rani, G., Jaswal, V., & Randhawa, J. S. (2020). Nano-bioremediation: a new age technology for the treatment of dyes in textile effluents. In *Bioremediation of Industrial Waste for Environmental Safety* (pp. 313-347).

Zamri, M. S. F. A., & Sapawe, N. (2019). Regeneration studies of TiO2 photocatalyst for degradation of phenol in a batch system. *Materials Today: Proceedings, 19*, 1327-1332.

Zhang, F., Wang, X., Liu, H., Liu, C., Wan, Y., Long, Y., & Cai, Z. (2019). Recent advances and applications of semiconductor photocatalytic technology. *Applied Sciences, 9*(12), 2489.

Zhang, H., & Chen, G. (2009). Potent antibacterial activities of Ag/TiO_2 nanocomposite powders synthesized by a one-pot sol− gel method. *Environmental science & technology, 43*(8), 2905-2910.

Zhu, J., Deng, Z., Chen, F., Zhang, J., Chen, H., Anpo, M. Zhang, L. (2006). Hydrothermal doping method for preparation of Cr^{3+}-TiO_2 photocatalysts with concentration gradient distribution of Cr^{3+}. *Applied Catalysis B: Environmental, 62*(3-4), 329-335.